COMPUTER SIMULATION OF A LARGE-SCALE NONLINEAR FEEDBACK CONTROL SYSTEM

by

Behshad Baseghi

Thesis submitted to the Graduate Faculty of the

Virginia Polytechnic Institute and State University

in partial fulfillment of the requirements for the degree of

MASTER OF SCIENCE

in

Electrical Engineering

APPROVED:

R. L. Moose, Chairman

J. A. Cadzow

H. F. VanLandingham

May 1978

Blacksburg, Virginia

ACKNOWLEDGMENTS

This thesis marks the end of another period in my education, yet it is a background for many more ambitious goals ahead.

Once it was accomplished, it was so easy to forget the hardships and frustrations that went along with its production. There were many who without their support and patience this would have been too difficult a task.

I would like to thank Dr. Richard L. Moose, the chairman of my committee, and Dr. Hugh F. VanLandingham, for their most valuable advice throughout the project. I would also like to extend my appreciation to Dr. James A. Cadzow, who was also a member of my committee, and Dr. Rick Johnson for his concern.

I must also thank and my brother, , and other friends for their assistance when most needed. I furthermore gratefully thank for her typing of this thesis.

TABLE OF CONTENTS

	Page
ACKNOWLEDGMENTS	ii
TABLE OF CONTENTS	iii
LIST OF FIGURES	iv
1.0 CIWS DIGITAL SIMULATION AND ANALYSIS	1
1.1 Introduction	1
1.2 Digital Simulation Approach (Fortran Version)	2
2.0 VERIFICATION SIMULATION OF NONLINEAR SAMPLED-DATA SYSTEMS WITH KNOWN RESPONSES	8
3.0 RESULTS	20
3.1 Simulation of Antenna Track Mode Block Diagram	23
4.0 CONCLUSIONS	44
REFERENCES	45
VITA	46
ABSTRACT	

LIST OF FIGURES

Figure No.	Title	Page
1.1	Linear Sampled-Data System.	4
2.1	Simulation of Nonlinearity.	9
2.2	Figure for Example 1.	10
2.3	A Closed-Loop Relay Control System for Example 1. .	13
2.4	Step-Response Variations.	14
2.5	Model of A Tracking System for Example 3.	15
2.6	Digital Model of Tracking System.	17
2.7	Error vs. Time for A Sample Interval T = .01 and A Small Noisy Input	18
2.8	Typical Tracking Error with Stochastic Excitation .	19
3.1	Output Angular Position with Noisy Input Sequences.	21
3.2	Output Angular Velocity with Motor Parameter Variations	22
3.3	Angular Position with Motor Mismatch.	24
3.4	Output Angular Velocity with Maximum Motor Mismatch	25
3.5	Output Angular Position with Maximum Motor Mismatch	26
3.6	Angular Position and Velocity	27
3.7	Output Angular Velocity, with Additive Noise, Mismatched Motors and T = .0005 Sec.	28
3.8	Angular Position.	29
3.9	Antenna Track Mode Block Diagram.	30
3.10	Cable Torque.	32
3.11	Angular Position.	33
3.12	Rate of Change of the Angular Position.	34

LIST OF FIGURES, cont.

Figure No.	Title	Page
3.13	"J. Hall" Output.	35
3.14	Cable Torque.	36
3.15	Angular Position.	37
3.16	Rate of Change of the Angular Position.	38
3.17	"J. Hall" Output.	39
3.18	Cable Torque.	40
3.19	Angular Position.	41
3.20	Rate of Change of Angular Position.	42
3.21	"J. Hall" Output.	43

1.0 CIWS DIGITAL SIMULATION AND ANALYSIS

1.1 Introduction

In the Department of Electrical Engineering at Virginia Polytechnic Institute and State University, an analysis of the CIWS gunfire control system was made. The analysis consisted of a digital simulation used to evaluate and check out the results of the hybrid computer.

For a continuous system of state equations we can derive a digital description that, with an appropriately chosen sampling interval, will accurately simulate the system. Indeed, in practical large scale systems, it is seldom the case that the actual differential equations can ever be solved to any anticipated degree of accuracy. In fact, nonlinear effects and system responses to random excitations can introduce noticeable difficulties that often invalidate the functional approximation techniques. Therefore, in a digital simulation, not only is a great deal of time and labor saved but also the degree of the approximation can be directly controlled by adjusting the speed of the sampling time. This direct method of solving the differential equations is very attractive as a simulation tool for large order systems with nonlinear dynamics. And, in addition, the decreased cost and availability of modern digital machines tend to emphasize this numerical approach. As a final comparison for the performance of the discrete time method, the analysis results of the Naval Close In Weapon System (CIWS) versus the data obtained by the hybrid computer is discussed in the following sections. This should provide a good comparison basis for both digital approaches.

1.2 Digital Simulation Approach (Fortran Version)

In practical applications it is not uncommon to find that input signals to a system cannot be described as specific functions of time. This can result, for example, when the input itself is the result of imperfect measurements such as RADAR data supplied to a tracking filter. In addition, physical forces can be present which are known only in terms of various observation averages such as wind-gust effects on an aircraft. Techniques have been developed which allow designers to account for system responses due to such random excitations when the system can be described by sets of linear differential equations [1-5]. A serious problem is encountered, however, if the major characteristics of the system are governed by nonlinear effects.

Methods of analysis for nonlinear systems with random inputs can be separated into three classes [6]:

(1) Quasi-linear methods are based on replacing a nonlinear element with a linear element chosen to approximate the behavior of the nonlinear element. A familiar design tool for control engineers which falls in this category is the describing function method [7].

(2) Functional methods such as Volterra's integral operators [8]. Applications of functional methods have been moderately successful but tend to provide unwieldy analytical techniques [6,8]. Both this and the previous method are analytic in nature in contrast with the numerical approach. It must be emphasized that only for a few meager types of nonlinear systems can an analytical approach even be used.

(3) Direct methods, i.e. a direct solution of the differential

equations. This last method has become increasingly more attractive as a simulation of nonlinear dynamics for large order systems. In a restricted class of problems, steady-state first- and second-order probability densities of signals within nonlinear systems can be calculated by solving the corresponding Fokker-Planck equations [9].

The approach taken in this report falls in this last category of direct methods and results in a large work reduction. First, a general approach is presented for simulation of nonlinear systems which are composites of linear subsystems and nonlinear memoryless effects when they are forced by random inputs. Second, the method is applied to three specific examples which provide a comparison with other solutions. As a practical view, second-order systems with a single nonlinearity are essentially at the analytical limit, especially when stochastic inputs are present. On the other hand, increased availability and decreased cost of computation have provided a resurgence of interest in simulation methods in general and in simulation of complex nonlinear feedback systems with stochastic excitations in particular.

This simulation technique is presented for systems which can be modeled as interactions of constant-parameter linear differential equations with nonlinear memoryless elements. Control system engineers have long been aware of "equivalent discrete-time" models for systems described by ordinary differential equations. For completeness, this development is included here. Fig. 1.1 illustrates a general linear sampled-data system. The sample-and-hold (clamp) approach is the simplest method of implementing the sampling of the inputs in addition to providing continuous-time excitation to the original system.

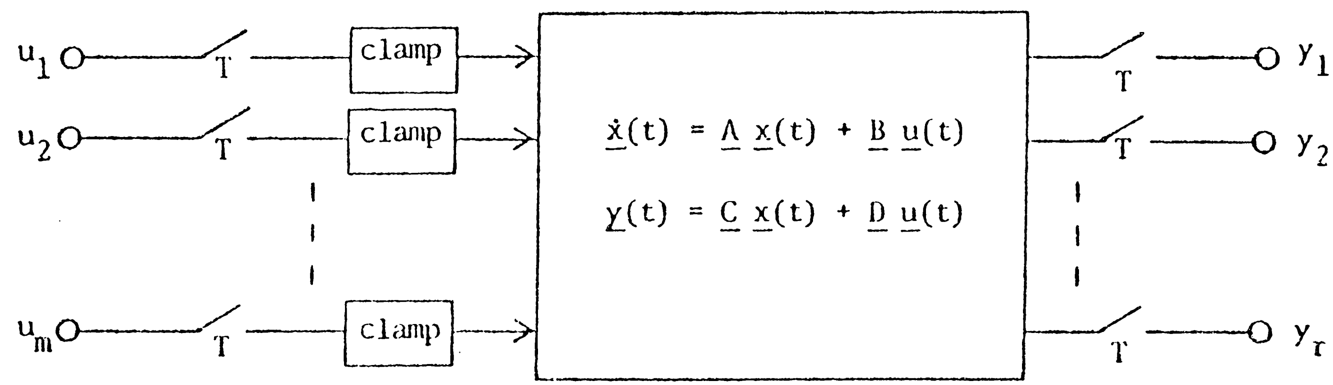

Fig. 1.1 Linear Sampled-Data System

Assuming the linear system of Fig. 1.1 is time-invariant and $\underline{x}(t_0)$ is known, the solution for $\underline{x}(t)$ in terms of $\underline{u}(t)$ is given by

$$\underline{x}(t) = \underline{e}^{\underline{A}(t-t_0)}\underline{x}(t_0) + \int_{t_0}^{t} \underline{e}^{\underline{A}(t-\tau)}\underline{Bu}(\tau)d\tau \qquad (1.2.1)$$

For $t_0 = nT$ and $t = nT+T$, where T is the clamp interval,

$$\underline{x}(nT+T) = \underline{e}^{\underline{A}T}\underline{x}(nT) + \int_{nT}^{nT+T} \underline{e}^{\underline{A}(nT+T-\tau)}\underline{Bu}(\tau)d\tau. \qquad (1.2.2)$$

If, as indicated in Fig. 1.1,

$$\underline{u}(t) = \underline{u}(nT) \quad \text{for } nT \leq t < nT+T \qquad (1.2.3)$$

for integer n, then letting $\lambda = nT+T-\tau$, (1.2.2) becomes

$$\underline{x}(nT+T) = \underline{e}^{\underline{A}T}\underline{x}(nT) + \int_0^T \underline{e}^{\underline{A}\lambda}\underline{B}d\lambda\underline{u}(nT). \qquad (1.2.4)$$

Also, by considering the outputs only at sample times,

$$\underline{y}(nT) = \underline{Cx}(nT) + \underline{Du}(nT). \qquad (1.2.5)$$

Equations (1.2.4) and (1.2.5) together comprise an equivalent discrete-time state model for the system of Fig. 1.1. Standard numerical techniques are available for the calculation of the coefficient matrices in (1.2.4); however, one useful approach is as follows.

In the discrete-time equivalent model (1.2.5) defines

$$\underline{\Phi}(T) = \underline{e}^{\underline{A}T} \quad \text{and} \quad \underline{\Gamma}(T) = \int_0^T \underline{e}^{\underline{A}t}\underline{B}dt. \qquad (1.2.6)$$

$\underline{\Phi}(T)$ is called the transition matrix. There are several matrix techniques for calculating $\underline{e}^{\underline{A}T}$ from a (constant, square) matrix $\underline{A}$. For second- and even third- and fourth-order systems, a closed-form can be obtained using Laplace transforms.

$$\underline{\Phi}(t) = \mathcal{L}^{-1}\{[s\underline{I} - \underline{A}]^{-1}\}. \tag{1.2.7}$$

For high-order systems a more convenient approach is to use the basic defining series for machine computation, i.e.

$$\underline{e}^{\underline{A}T} = \underline{I} + \underline{A}T + \frac{T^2}{2!}\underline{A}^2 + \ldots + \frac{T^k}{k!}\underline{A}^k + \ldots \quad . \tag{1.2.8}$$

The definition given in (1.2.8) provides a basic computer-oriented approach to the calculation of $\underline{\Phi}(T)$. In addition, the equivalent input matrix $\underline{\Gamma}(T)$ from (1.2.6) is

$$\underline{\Gamma}(T) = \int_0^T \underline{e}^{\underline{A}t}\,dt\underline{B}. \tag{1.2.9}$$

The integral portion of (1.2.9), when applied to (1.2.8) term-by-term, results in the series form

$$\underline{\Gamma}(T) = \{T\underline{I} + \frac{T^2}{2!}\underline{A} + \frac{T^3}{3!}\underline{A}^2 + \ldots + \frac{T^k}{k!}\underline{A}^{k-1} + \ldots\}\underline{B}. \tag{1.2.10}$$

The digital computer is well adapted to performing the indicated operations of (1.2.8) or (1.2.10); however, if the series

$$\underline{M}(T) = T\underline{I} + \frac{T^2}{2!}\underline{A} + \frac{T^3}{3!}\underline{A}^2 + \ldots \quad . \tag{1.2.11}$$

is first computed (for a given $\underline{A}$ and T); then

$$\underline{\Phi}(T) = \underline{I} + \underline{A}\cdot\underline{M}(T), \tag{1.2.12}$$

and

$$\underline{\Gamma}(T) = \underline{M}(T)\underline{B}. \tag{1.2.13}$$

Using the approach (1.2.11), (1.2.12) and (1.2.13), the first step is to determine $\underline{M}(T)$. Given $\underline{A}$, a T must be selected (according to accuracy desired in approximating $\underline{u}(t)$ and the first several terms of (1.2.11) must be calculated and summed.

A useful convergence test to determine when a sufficient number of terms of (1.2.11) has been taken is to compare the next term (matrix) entry-by-entry with the calculated partial sum so that the entries of the partial sum are changed by less than some percent error by the addition of the next term. Typically, for reasonable sample times T, ten to fifteen terms provide accuracy well within .01%; however, a sophisticated routine should have a check on the error. The series (1.2.8) or (1.2.11) is mathematically well behaved, i.e. the factorial factor in the denominator helps to provide rapid convergence; but if convergence fails even after 25 terms, the error tolerance may be too tight. Division by 25! is in excess of 10^{25}; thus, if the error is too high after 25 terms, the problem may require a reduction of T.

2.0 VERIFICATION SIMULATION OF NONLINEAR SAMPLED-DATA SYSTEMS WITH KNOWN RESPONSES

In the modeling of separate components of a physical system it is often necessary to account for some nonlinearity such as amplifier saturation, dead-zone of gears, nonlinear friction, and so on. A convenient technique again uses the idea of clamping. If a memoryless nonlinearity N, as shown in Fig. 2.1a, occurs in the system structure, and artificial "induced" sampling and clamping can be added, as in Fig. 2.1b, it is easily demonstrated that the variation y_c follows that of y as a piecewise constant approximation and that

$$\lim_{T\to 0} |y_c(t) - y(t)| \to 0 \qquad (2.1)$$

uniformly with T.

The clamp outputs are taken as part of the composite state vector. At the sample instants the output of an induced clamp is held constant at the value N[x(nT)], (see Fig. 2.1b). That is, the sampled signal is mapped by the nonlinearity into the value which is clamped.

<u>Example 1.</u> Fig. 2.2 shows a sampled-data system with nonlinear damping. The unit-step response will be simulated.

From the signal diagram of Fig. 2.2b the following relations are found:

$$\dot{\underline{x}} = A\underline{x} = \left[\begin{array}{ccc|cc} 0 & 1 & 0 & 0 & 0 \\ -4 & 0 & -1 & 1 & 0 \\ 0 & 0 & 0 & 0 & 0 \\ \hline 0 & 0 & 0 & 0 & 0 \\ 0 & 0 & 0 & 0 & 0 \end{array}\right] \underline{x}, \quad nT < t < (n+1)T \qquad (2.2)$$

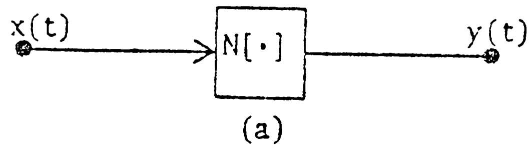

(a) Nonlinear, Memoryless Device

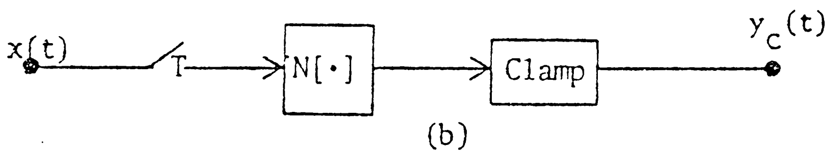

(b) Induced Sample and Clamp for Nonlinearity

Fig. 2.1 Simulation of Nonlinearity

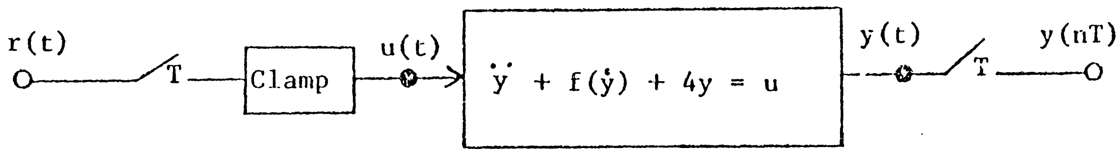

(a)

Nonlinear Sampled-Data System

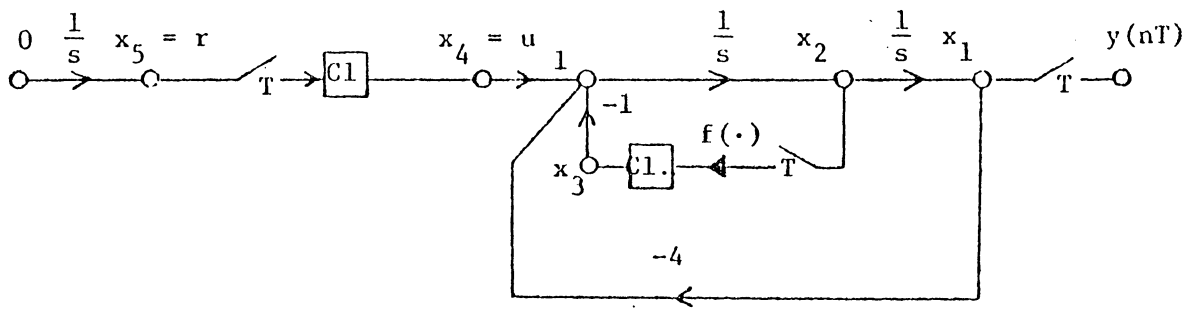

(b)

Detailed Diagram for Step-Response

Fig. 2.2 Figure for Example 1

$$x(nT^+) = J[\underline{x}(nT^-)] = \left[\begin{array}{ccc|cc} 1 & 0 & 0 & 0 & 0 \\ 0 & 1 & 0 & 0 & 0 \\ 0 & f(\cdot) & 0 & 0 & 0 \\ \hline 0 & 0 & 0 & 0 & 1 \\ 0 & 0 & 0 & 0 & 1 \end{array}\right] \underline{x}(nT^-), \quad n=0,\ 1,\ \ldots \tag{2.3}$$

Equations (2.5) and (2.3) represent, respectively, the continuous-time dynamics between sample times and the effects of resetting variables at the sample times. The unorthodox notation used in (2.3) means that $x_3(nT^+) = f(x_2(nT^-))$. In the subsequent examples these two effects will be combined at each sample time. Thus, if $\Phi(T)$ has been calculated for (2.5) and $x(nT^-)$ is known, then

$$x(nT^+) = J[x(nT^-)] \tag{2.5}$$

and

$$x((n+1)T^-) = (T)J[x(nT^-)] \tag{2.5}$$

That is, the overall transition is $\Phi(T)J[\cdot]$, where the J-operation accounts for the nonlinear elements. Notice that in this example the step-input was simulated as part of the system to avoid calculation of the input matrix $\Gamma(T)$.

In this section, it is demonstrated that relatively simple physical problems can be virtually intractable analytically, and yet not prove difficult by the present method.

Example 2. A Relay Control System

Although many references are available on techniques for solving nonlinear differential equations, there are pitifully few for which convenient closed-form solutions exist. Even so, a fundamental understanding can be obtained from a study of phase-plant trajectories for second-order systems. Kuo [10] has provided such an analysis for the calculation of the unit-step response of a relay control system. A diagram for this system is given in Fig. 2.3. A detailed phase-plane construction was used in [11] to find the unit-step response of Fig. 2.4a. Identical results were obtained by the present method. Also, it was a simple matter to alter the sample-time T to investigate its effect. The effect is to reduce the oscillation amplitude significantly as shown in Fig. 5b. Furthermore, the system can now be analyzed with noise present, as given in Fig. 2.4c, where the difference is a superimposed white noise of σ = 0.6 on the input step-function. It is interesting to see the effects of the additional stochastic input. Such simulations can be used to estimate the mean and variance of the output for a given stochastic input--a problem which is beyond exact analysis!

Example 3. A Tracking System

The third example, taken from [6], is diagrammed in Fig. 2.5. This example is the simulation of a simple feedback structure which can track constant velocity inputs. As part of the model, the saturation nonlinearity is required to reflect a limit on the output velocity. It is desired to determine both the transient response of the output y(t) and the mean value of the system error s(t)-y(t). The input consists of a ramp input s(t) = 40t and a superimposed stationary, first-order Markov random signal n(t) representing e.g. errors in the process of measuring the position s(t). The addition of the noise process makes the computation of the mean value of the error signal analytically impossible for

10

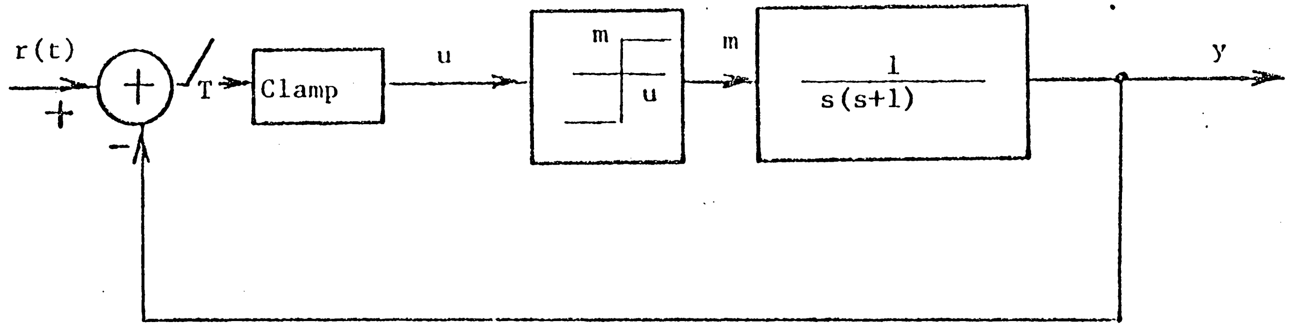

Fig. 2.3 A Closed-Loop Relay Control System for Example 1

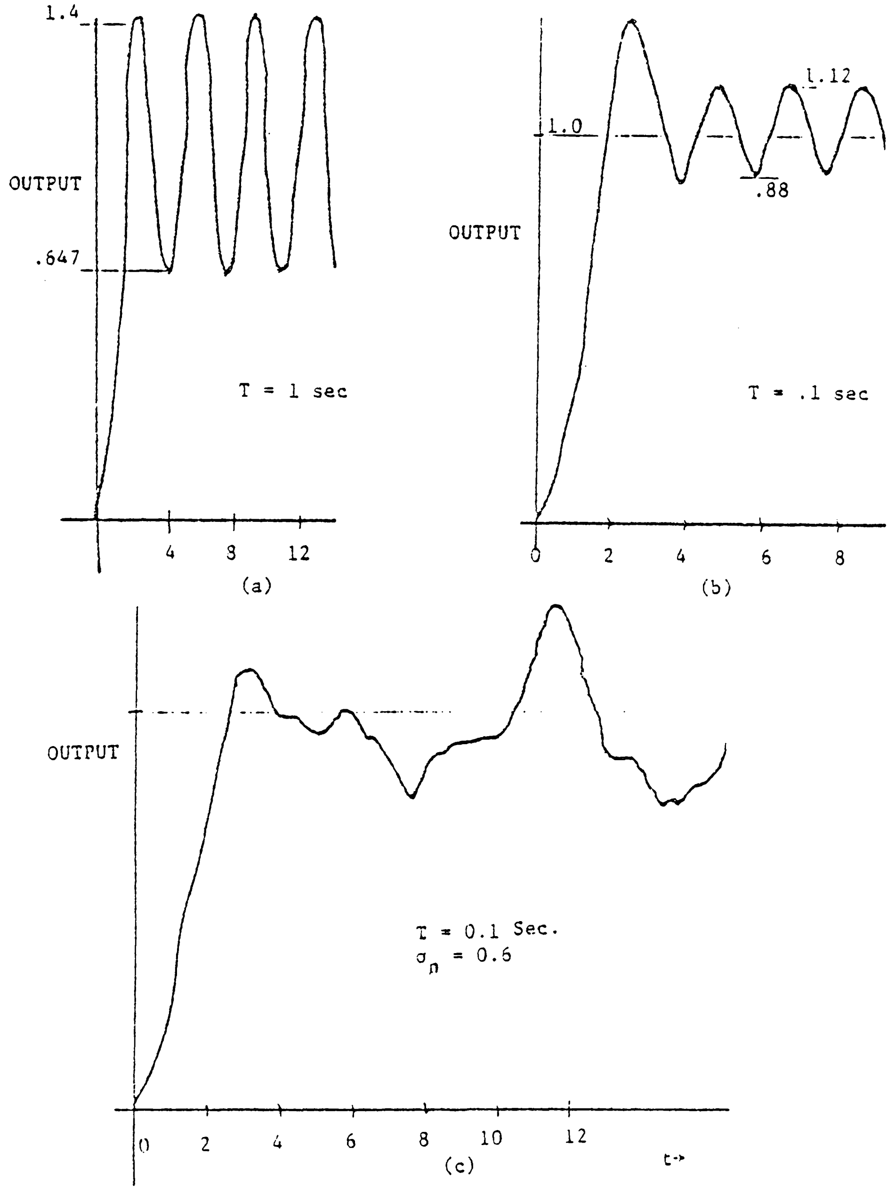

Fig. 2.4 (a) Step-Response(T=1), (b) Step-Response(T=0.1),
(c) Response to Unit-step plus white noise of σ=0.6

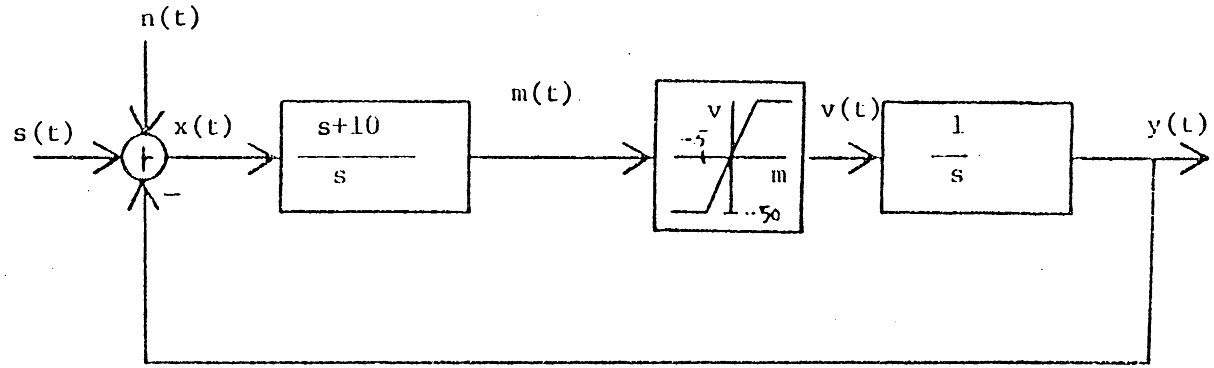

Fig. 2.5 Model of A Tracking System for Example 3

the feedback problem. Results in [6] are known only from analog simulation techniques and quasi-piecewise linear approximations. The digital simulation shown in Fig. 2.6 can be represented by the following set of equations for $t_k < t < t_{k+1}$.

$$\dot{\underline{x}}(t) = \begin{bmatrix} 0 & 1 & 0 & 0 & 0 \\ 0 & 0 & 0 & 0 & 0 \\ -10 & 0 & 0 & 10 & 0 \\ 0 & 0 & 0 & 0 & 1 \\ 0 & 0 & 0 & 0 & 0 \end{bmatrix} \underline{x} + \begin{bmatrix} 0 \\ 0 \\ 10 \\ 0 \\ 0 \end{bmatrix} n(t) \qquad (2.6)$$

and at $t = t_k$ the jump matrix (J) becomes

$$\underline{x}_k^+ = \begin{bmatrix} 1 & 0 & 0 & 0 & 0 \\ N & [m^- - x_1^- + x_3^- + x_4^-] & & & \\ 0 & 0 & 0 & 0 & 0 \\ 0 & 0 & 0 & 1 & 0 \\ 0 & 0 & 0 & 0 & 1 \end{bmatrix} \underline{x}_k^- \qquad (2.7)$$

where N[·] is the nonlinearity in Fig. 2.6.

Results shown in Fig. 2.7 indicate that the error, when n(t) = 0, approaches zero with increasing time. The values are nearly identical to those of reference [6] and are obtained with a significant reduction of effort. Fig. 2.8 shows a typical error output when N(t) is added to the system input.

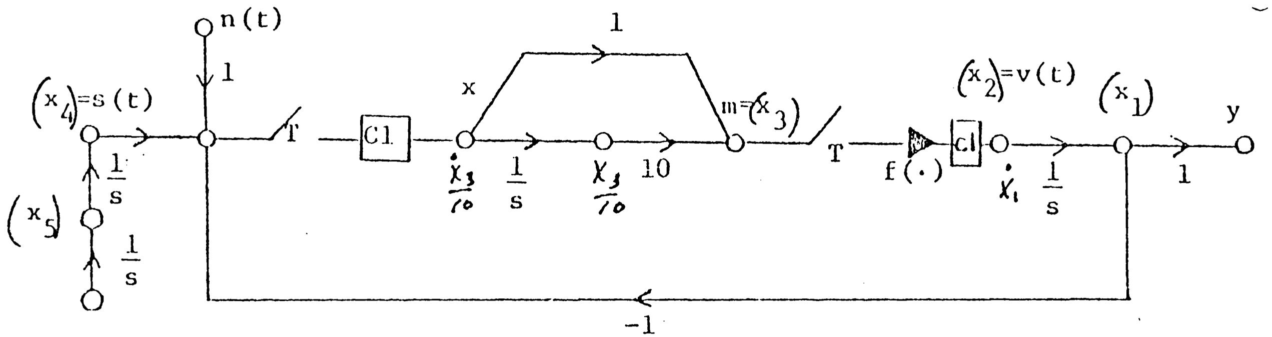

Fig. 2.6 Digital Model of Tracking System

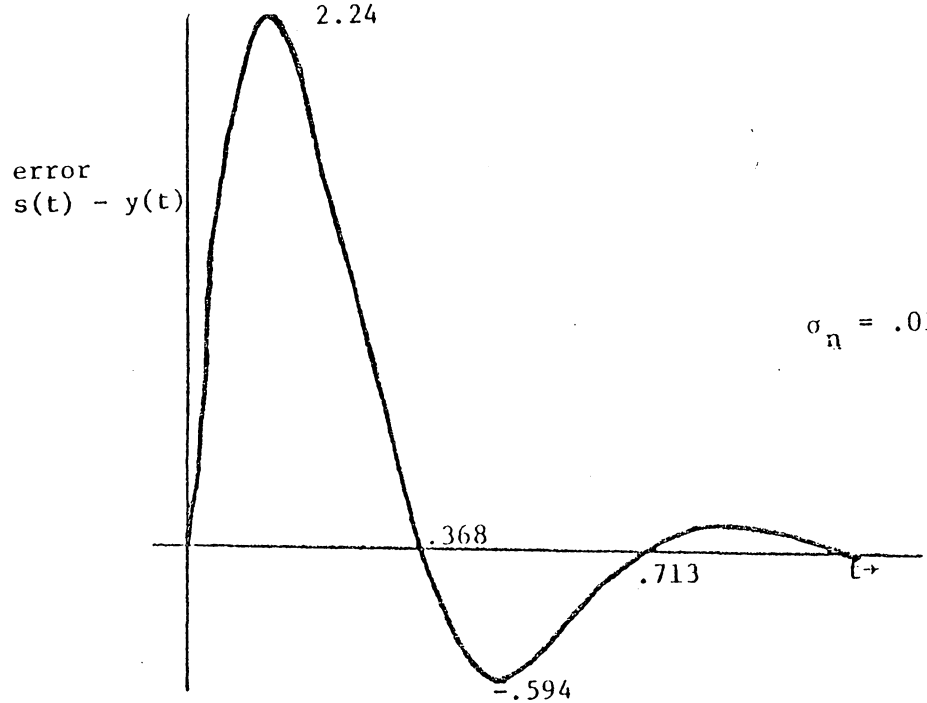

Fig. 2.7 Error vs. Time for A Sample Interval T = .01 and A Small Noisy Input

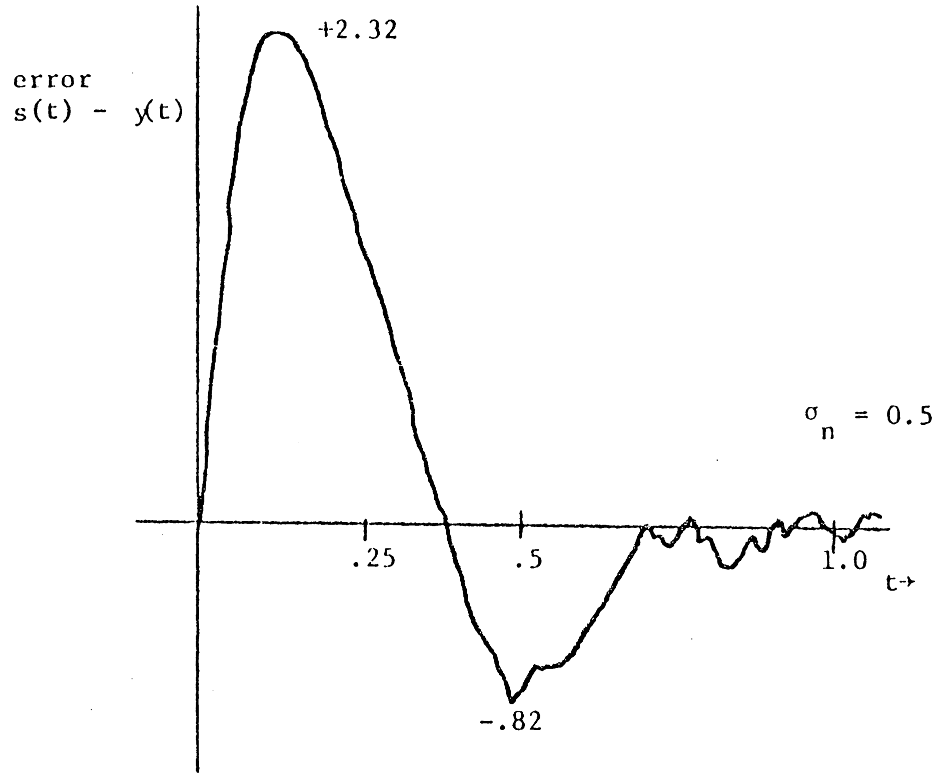

Fig. 2.8 Typical Tracking Error with Stochastic Excitation

3.0 RESULTS

A digital simulation of the entire system shown in Fig. 2.8 was written in Fortran for use on the IBM 370 computing system. It was found that, due to the short word length of the 370 system and the design of the lightly damped right and left motors, each of which contain several nonlinearities, that double precision was necessary. It should be noted that this would correspond very closely to single precision of the CDC computing system used at the Dahlgren Laboratory.

The first runs made on the system revealed the lightly damped nature of the main control motors. A linear, and then a nonlinear, analysis demonstrated the rapid response and high overshoots of the individual motors. However, due to matching and a good system design, the output responses, angular rate as shown by Z_8, and angular position as shown by Z_9 in Fig. 2.8 was not affected that much by large overshoots in angular rate.

A sample interval of one millisecond or less was selected with the system rate input set equal to zero, and zero-mean white Gaussian noise of standard deviation .05 applied. It was also decided to drive the system with additive noise of variance $\sigma^2 = 1$ amp^2 added directly to the ±9 amp current offsets. The results of output angular position show mount motion of less than 2.5 milliradians in Fig. 3.1.

An examination of system response to the input sequence command of: 0.0, for $0 \leq t \leq 1$ sec; .1, for $1.0 \leq t \leq 2$ sec. Then 0.0 for $t < 2$ sec was made with tolerance variation of ±1% in the right and left motor feedback (6000) parameter, and ±1.5% in the (3) parameter of Fig. 2.8. Resulting angular velocity is shown in Fig. 3.2 and angular position in

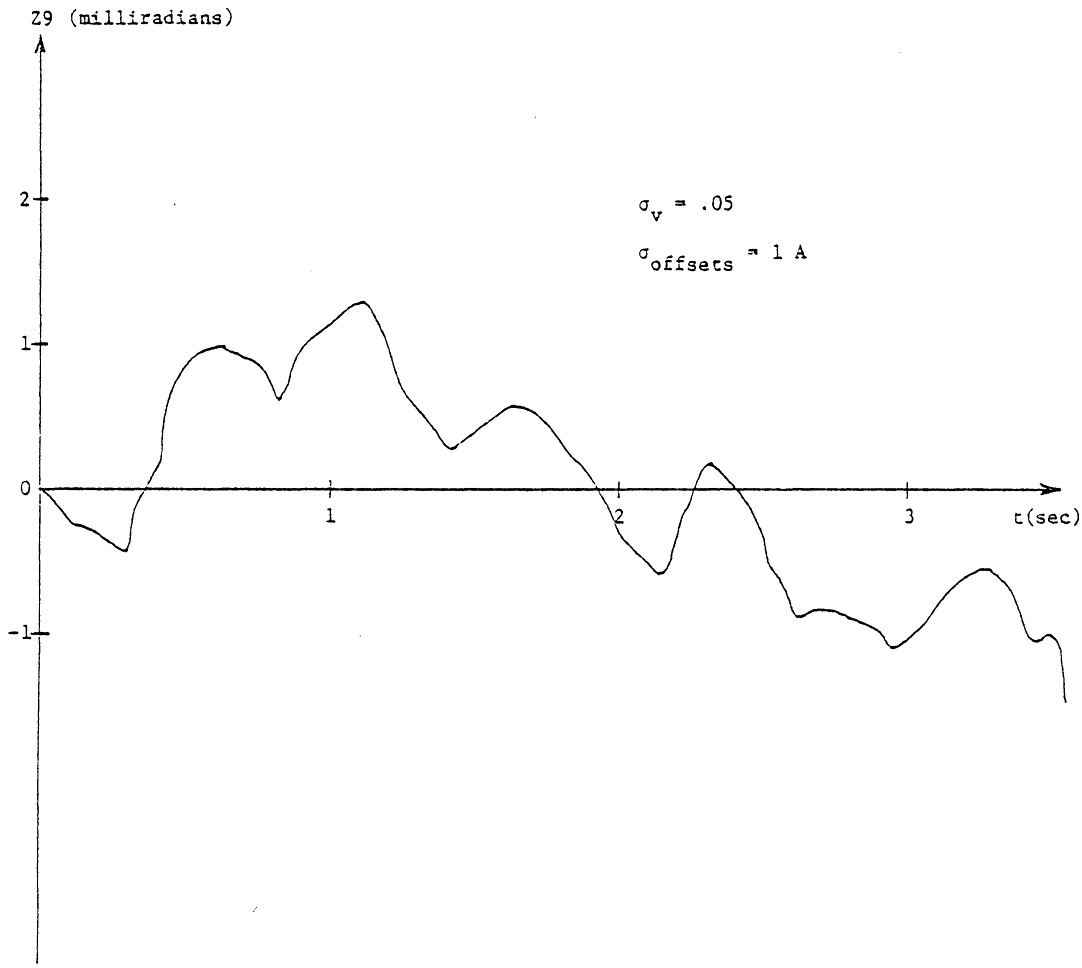

Fig. 3.1 Output Angular Position with Noisy Input Sequences

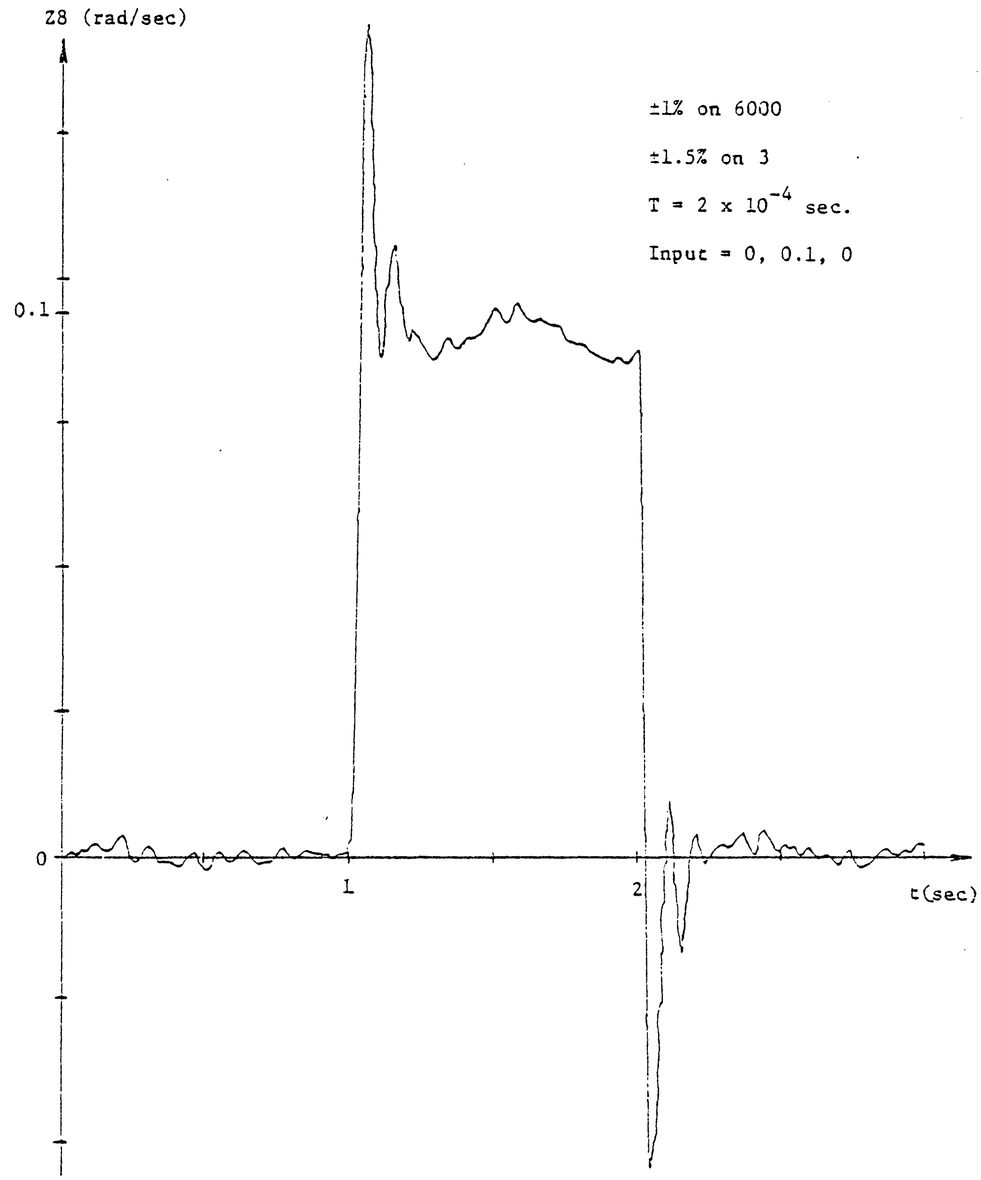

Fig. 3.2 Output Angular Velocity with Motor Parameter Variations

Fig. 3.3. The next set of runs were made using information supplied by Bob Palmer of NSWC, White Oak, Maryland. They show output angular rate, Fig. 3.4, and angular position, Fig. 3.5, when the maximum manufacture tolerances of ±5% on Jm, and ±10% on KT (motor mechanical parameters) were used. In addition, the previous command sequences of 0.0, 0.1, 0.0, the previously described input noises of σ = .05 and σ = 1 amp were applied. Results show little change and a very good output angular position response.

At this time, an input sequence of 0.0, +0.10, 0.0 and -0.1 was applied to the closed loop mount controller. The motor parameters were matched and additive noise was applied to simulate random ship motion. The standard deviation was again 0.05 at the system input and 1.0 amp at the ±9 amp current offset inputs. The results shown in Fig. 3.6 clearly indicate that output mount position does return to 0.0 after the last input control step.

Results shown in Figs. 3.7 and 3.8 show mount response with the same sequence applied except that the final command of -0.1 rad/sec is held for $t \geq 3.0$ seconds. Noise of the same standard deviations as before has been applied, and, in addition, the motors have again been mismatched ±5% for Jm and ±10% for KT. The sampling interval was increased to .0005 seconds in order to conserve computational time.

3.1 Simulation of Antenna Track Mode Block Diagram

The output of the gun-fire control system is used for the Antenna Track Mode. The digital simulation of the block diagram of the antenna shown in Fig. 3.9 yielded a close duplicate of the results provided by

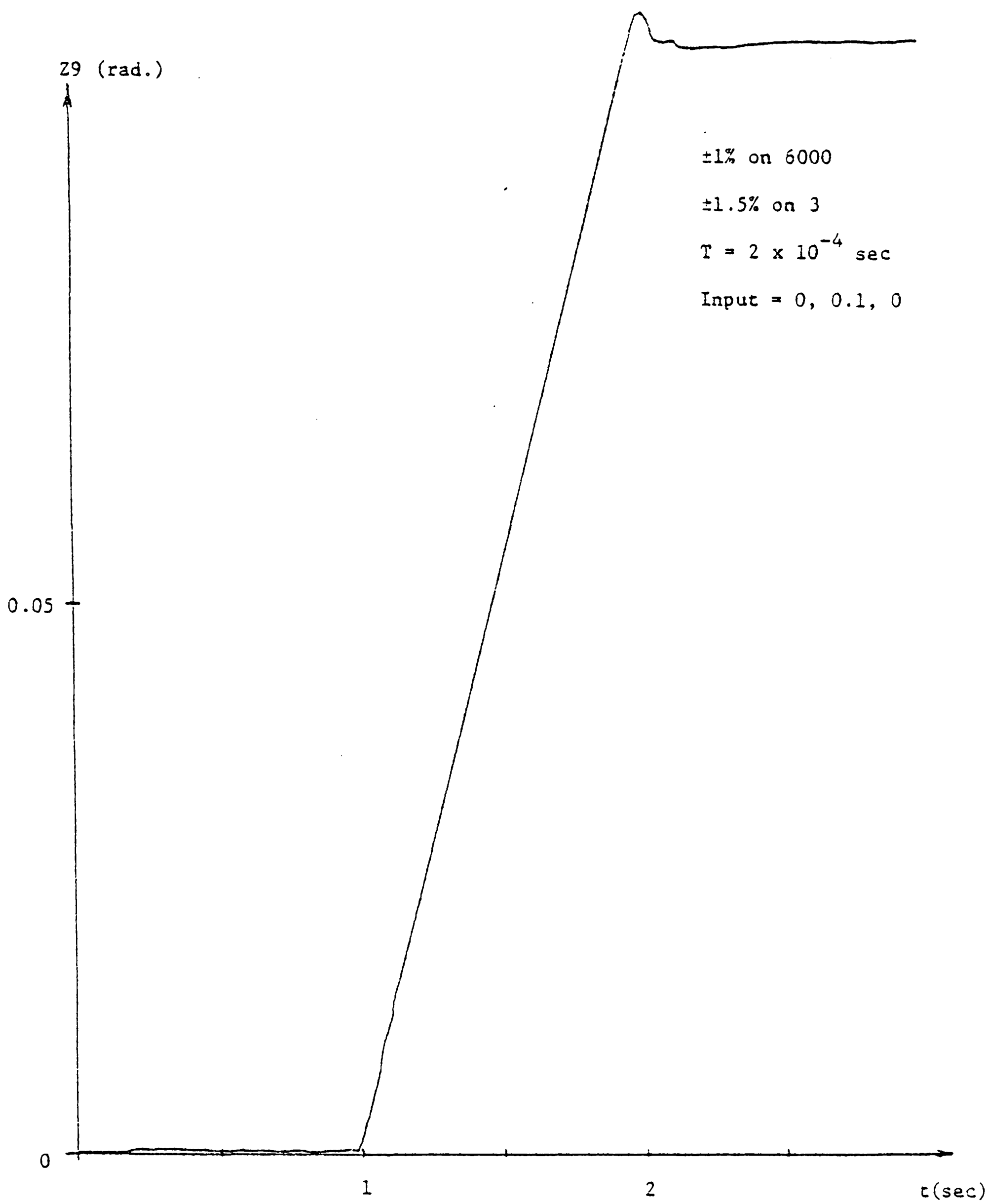

Fig. 3.3 Angular Position with Motor Mismatch

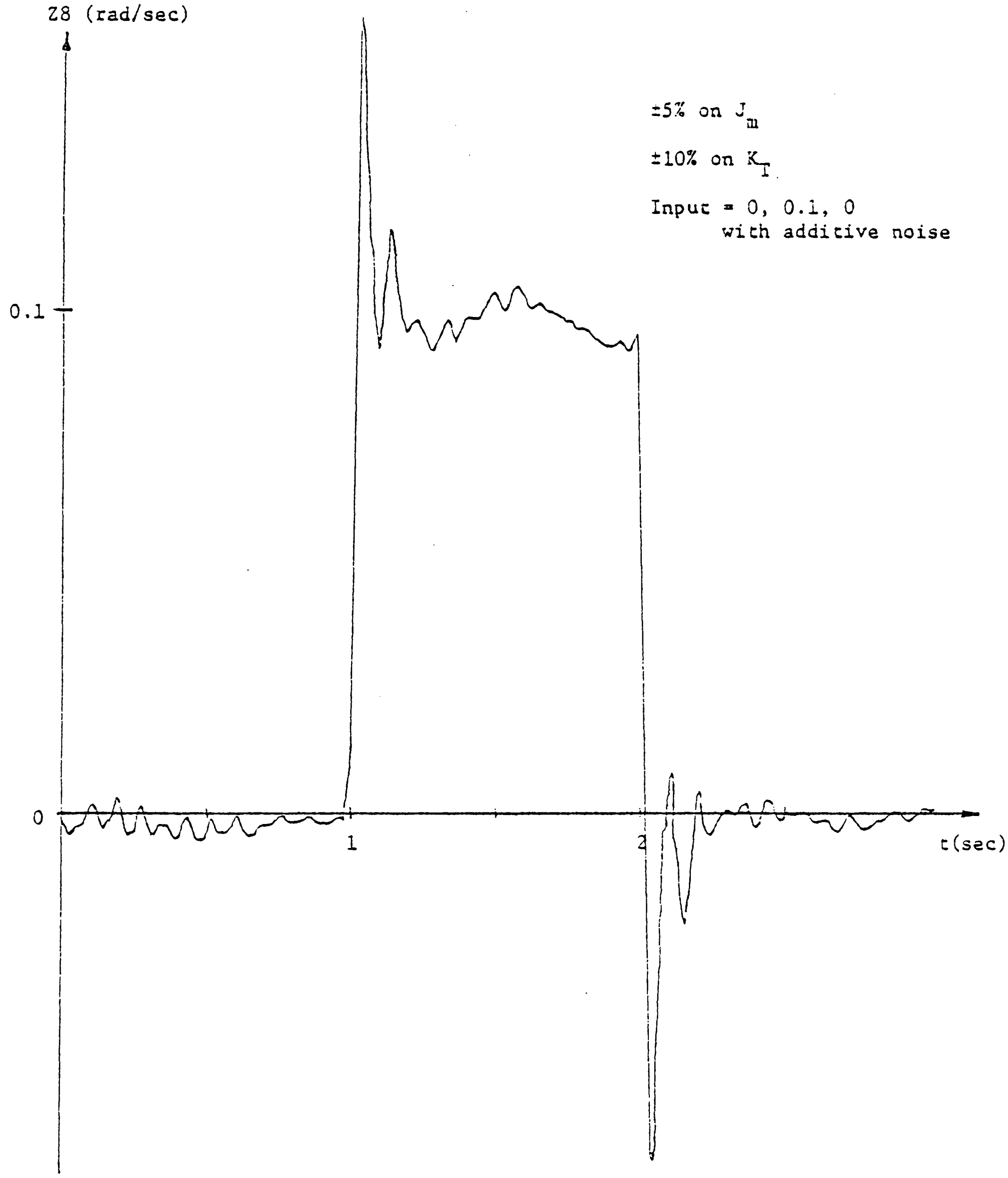

Fig. 3.4 Output Angular Velocity with Maximum Motor Mismatch

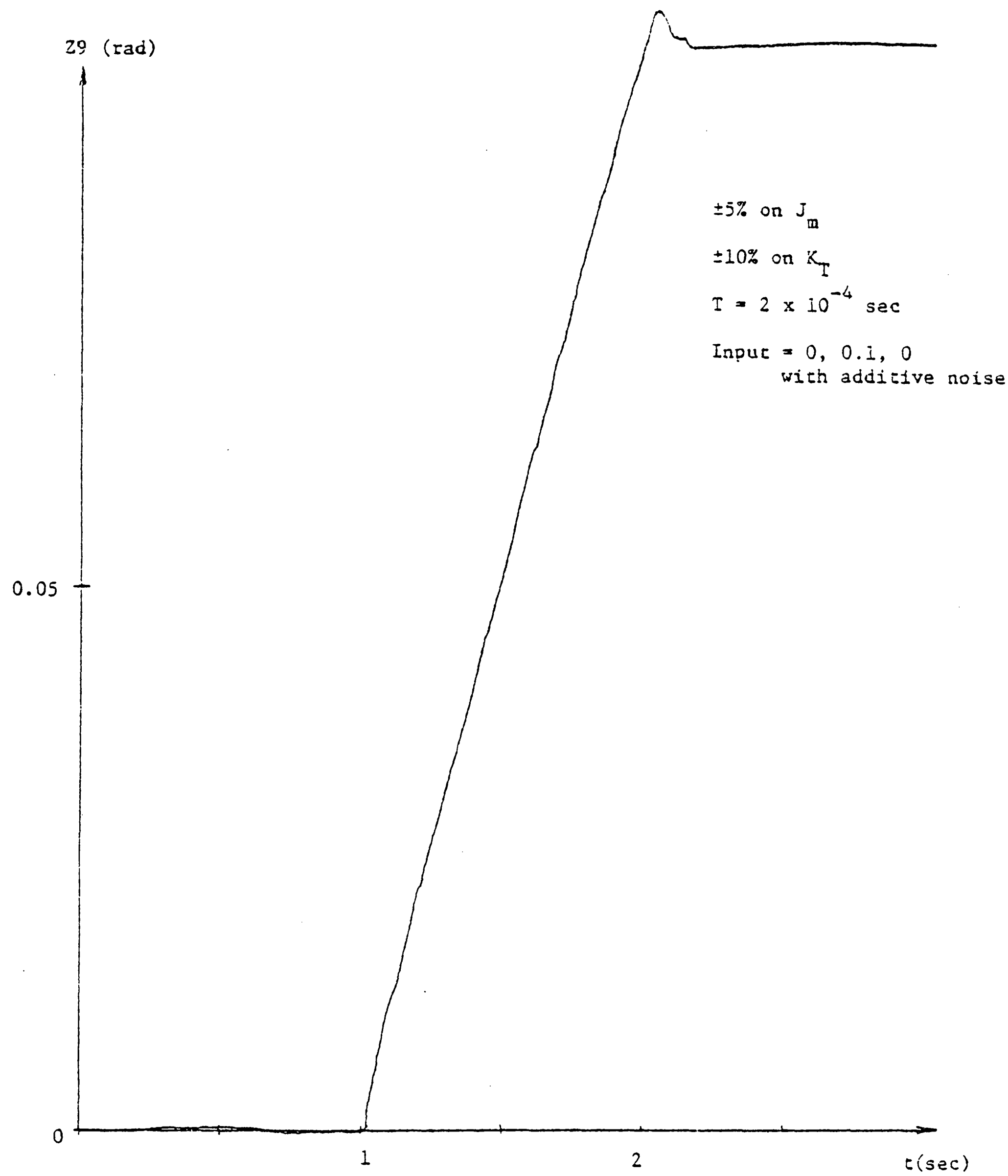

Fig. 3.5 Output Angular Position with Maximum Motor Mismatch

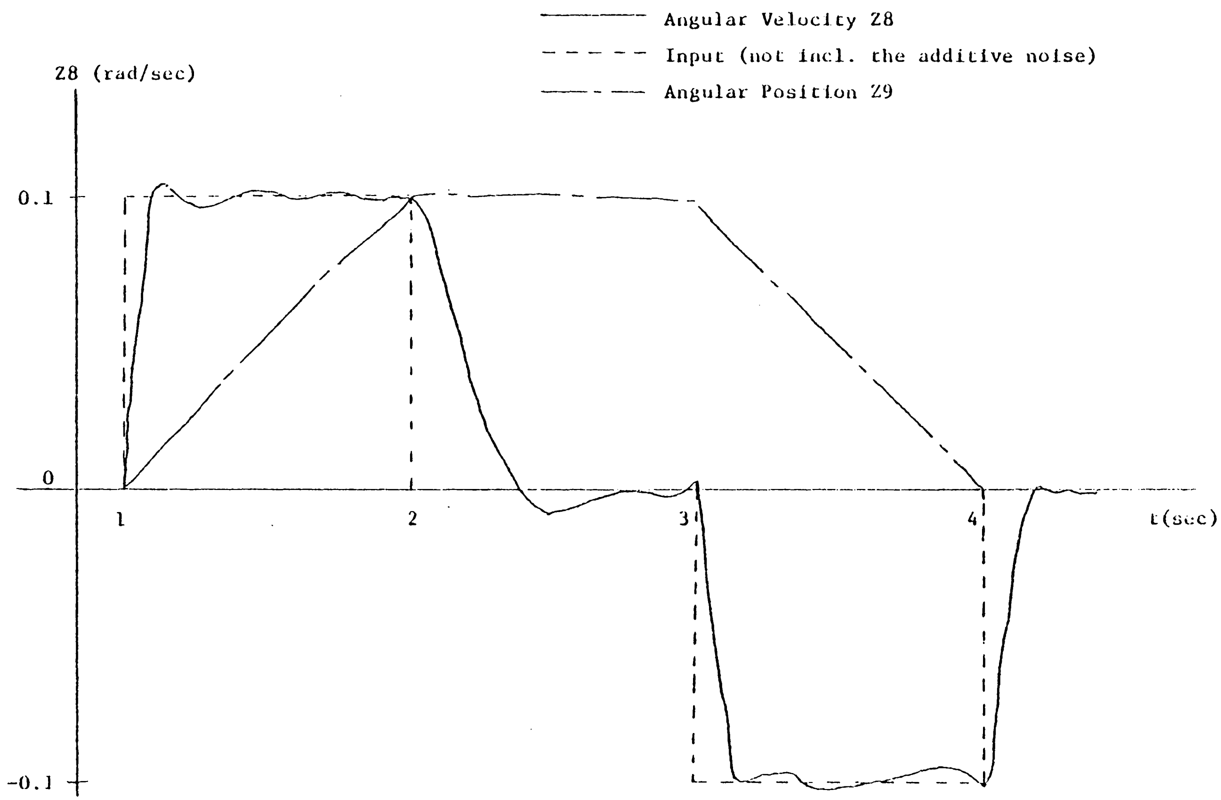

Fig. 3.6 Angular Position and Velocity

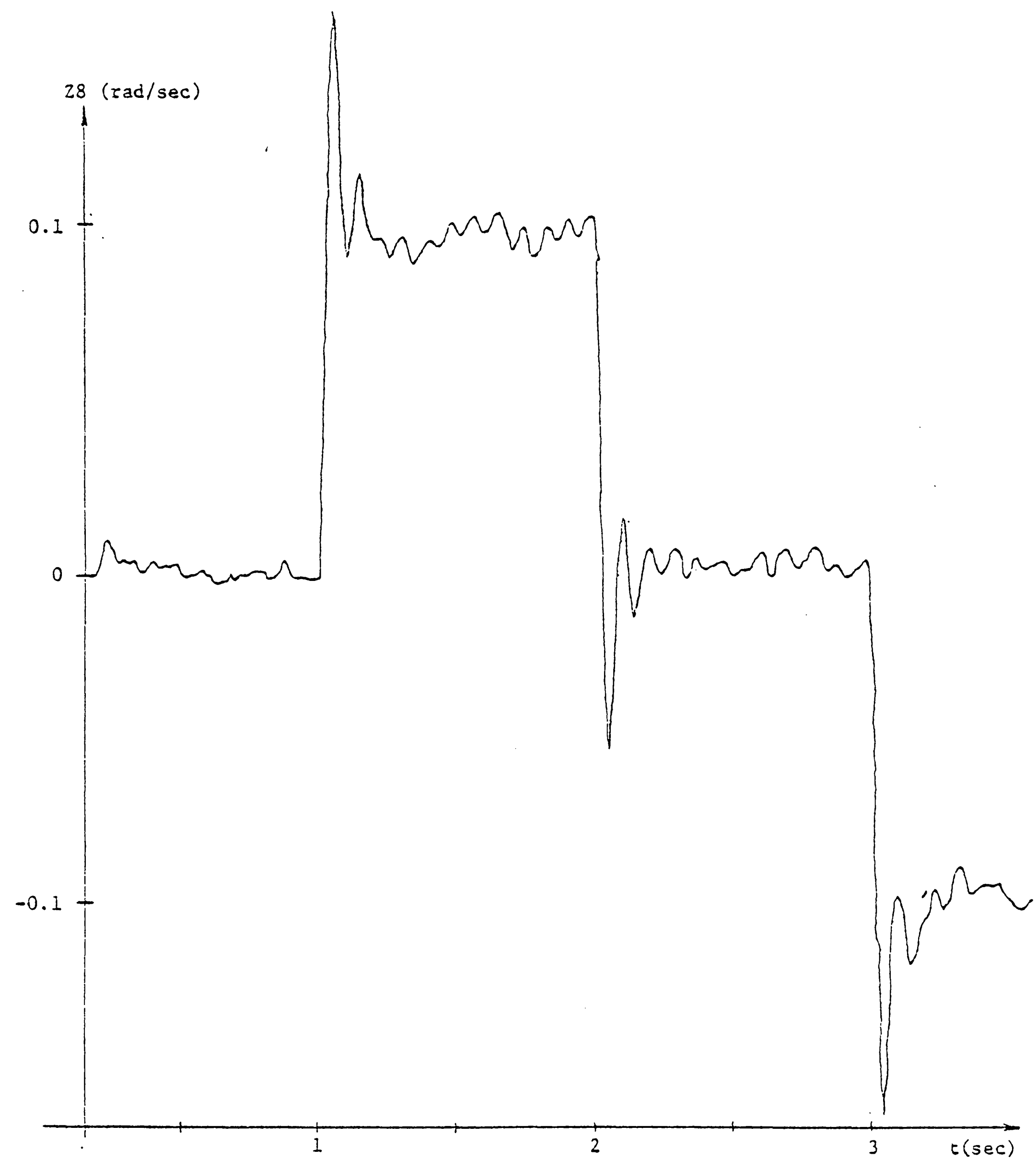

Fig. 3.7 Output Angular Velocity, with Additive Noise, Mismatched Motors and T = .0005 Sec.

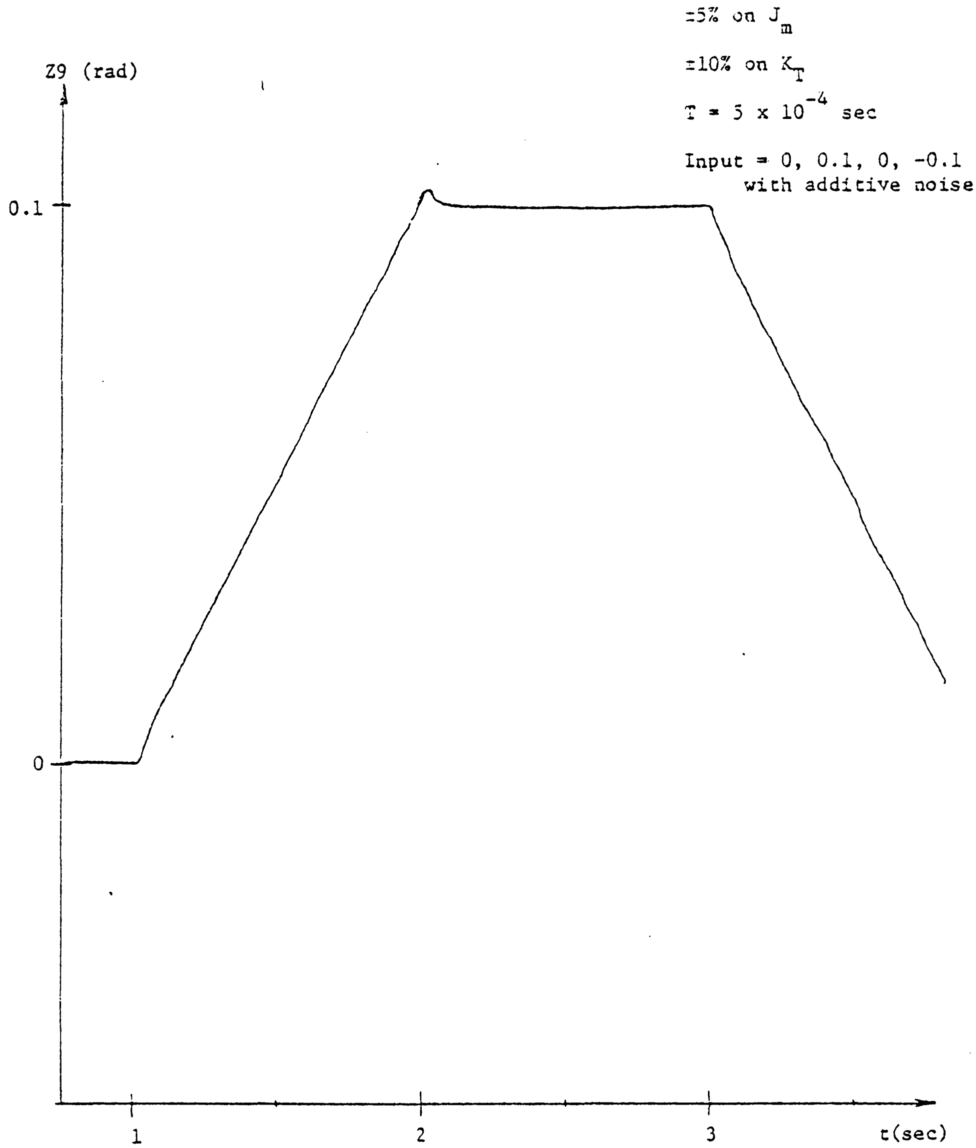

Fig. 3.8 Angular Position

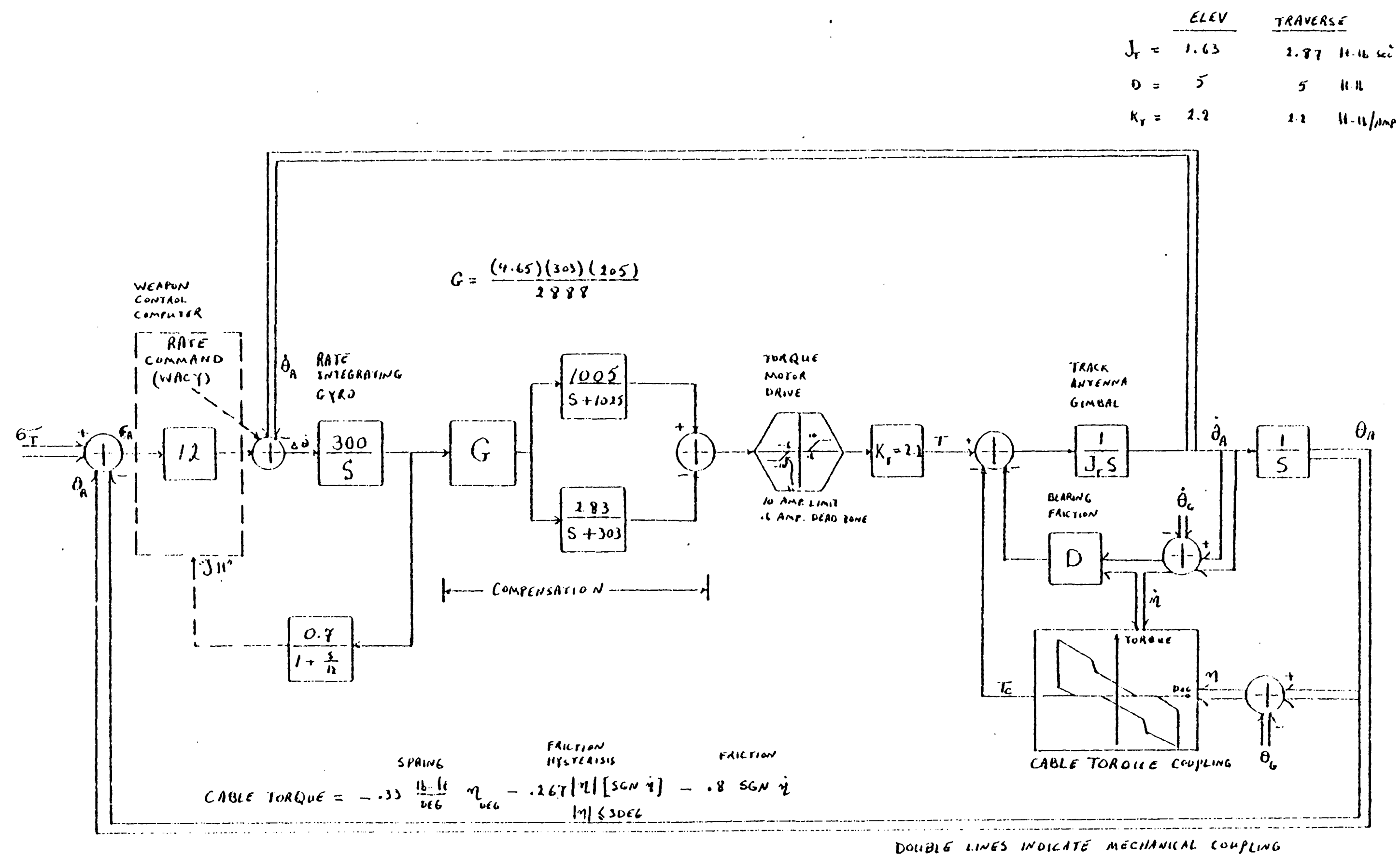

Fig. 3.9 Antenna Track Mode Block Diagram

the hybrid computer.

Setting ε_A equal to zero by breaking the feedback loop and assuming that the forcing function of the system is the "WACY" input, and furthermore, disconnecting the $\dot{\theta}_G$ and θ_G inputs, the results in figure set 3.10 through 3.13 will be obtained.

In this case the "WACY" command was 0.5 rad/sec for one second and 0.0 rad/sec for the next second and -0.5 rad/sec for the following second. Initially, it was assumed that the system was at rest, i.e., every state variable was set to zero.

The next results, shown in Figs. 3.14 through 3.17, are obtained when the feedback loop is reconnected and a gain block equal to an amplification of 12 is put in the loop. Again, disconnecting the outputs of the gun-mount system, i.e. θ_G and $\dot{\theta}_G$, and letting σ_T take on the values of 0.06 rad/sec and 0.0 and -0.06 rad/sec, with the "WACY" input assuming the previous set values.

The last set of results, Figs. 3.18 through 3.21, result when σ_T assumes the values of 0.120 rad and 0.0 and -0.120 rad while the "WACY" input is as before, i.e. 0.5, 0, -0.5. Note that in this case the "cable torque" was not disconnected.

The sampling interval for all the simulations was chosen to be 0.001 second. This led to a stable simulation for each set of experiments.

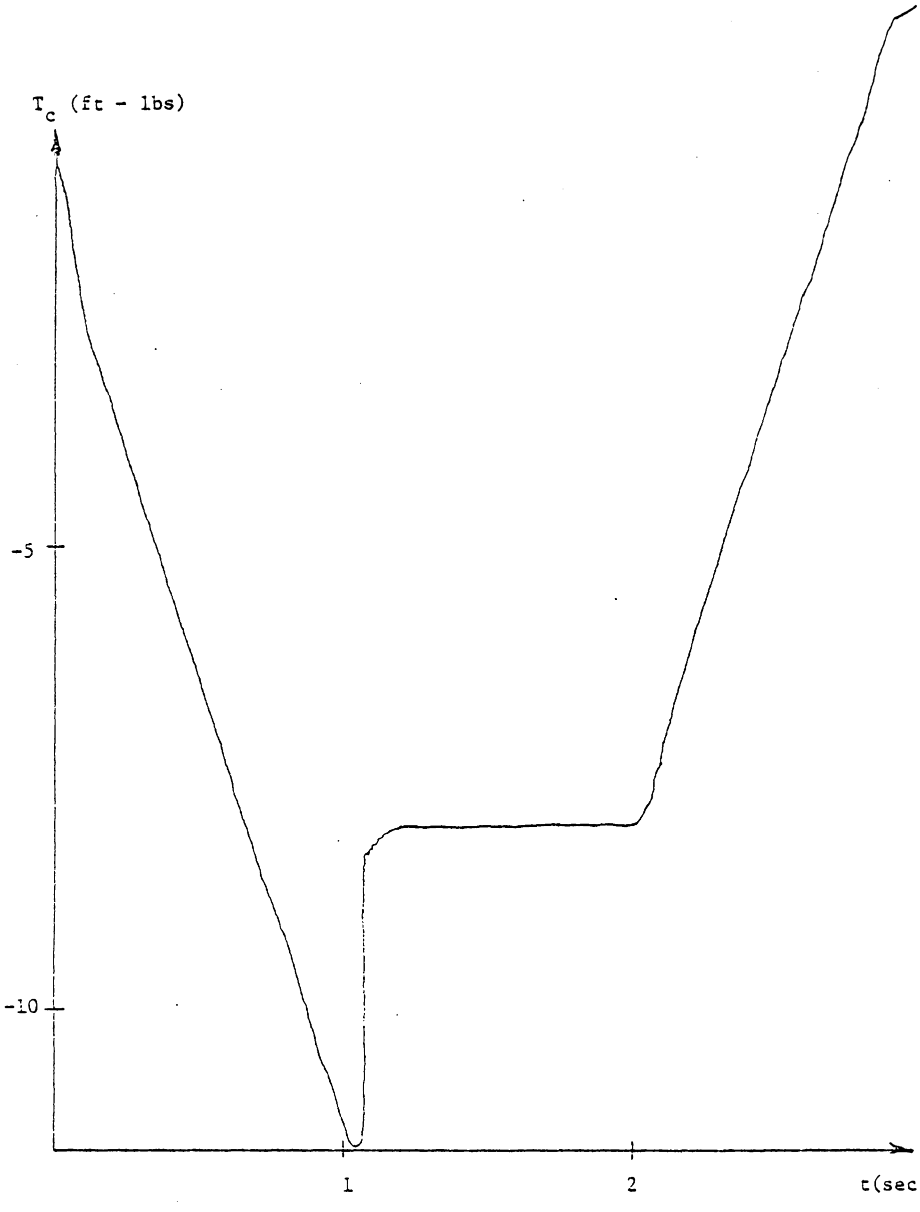

Fig. 3.10 Cable Torque

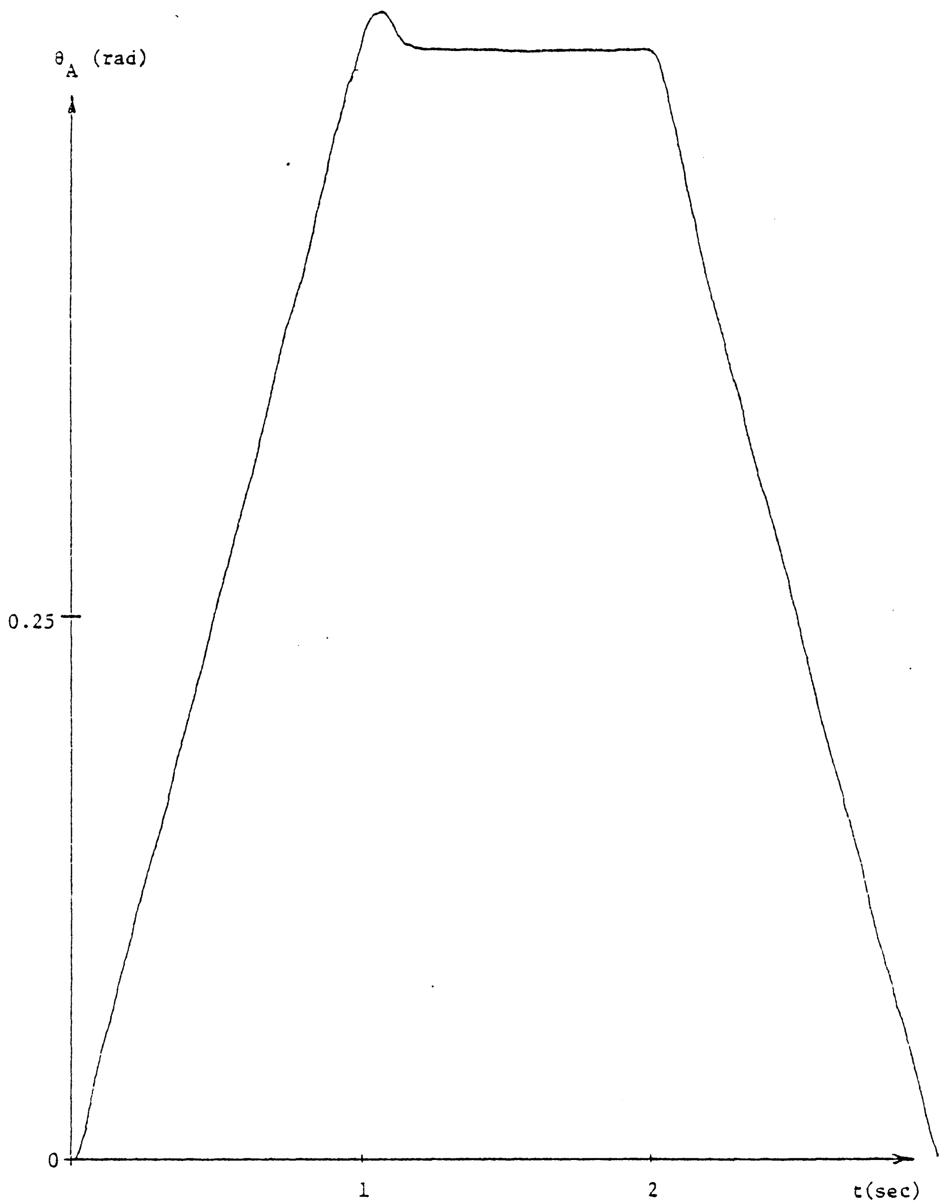

Fig. 3.11 Angular Position

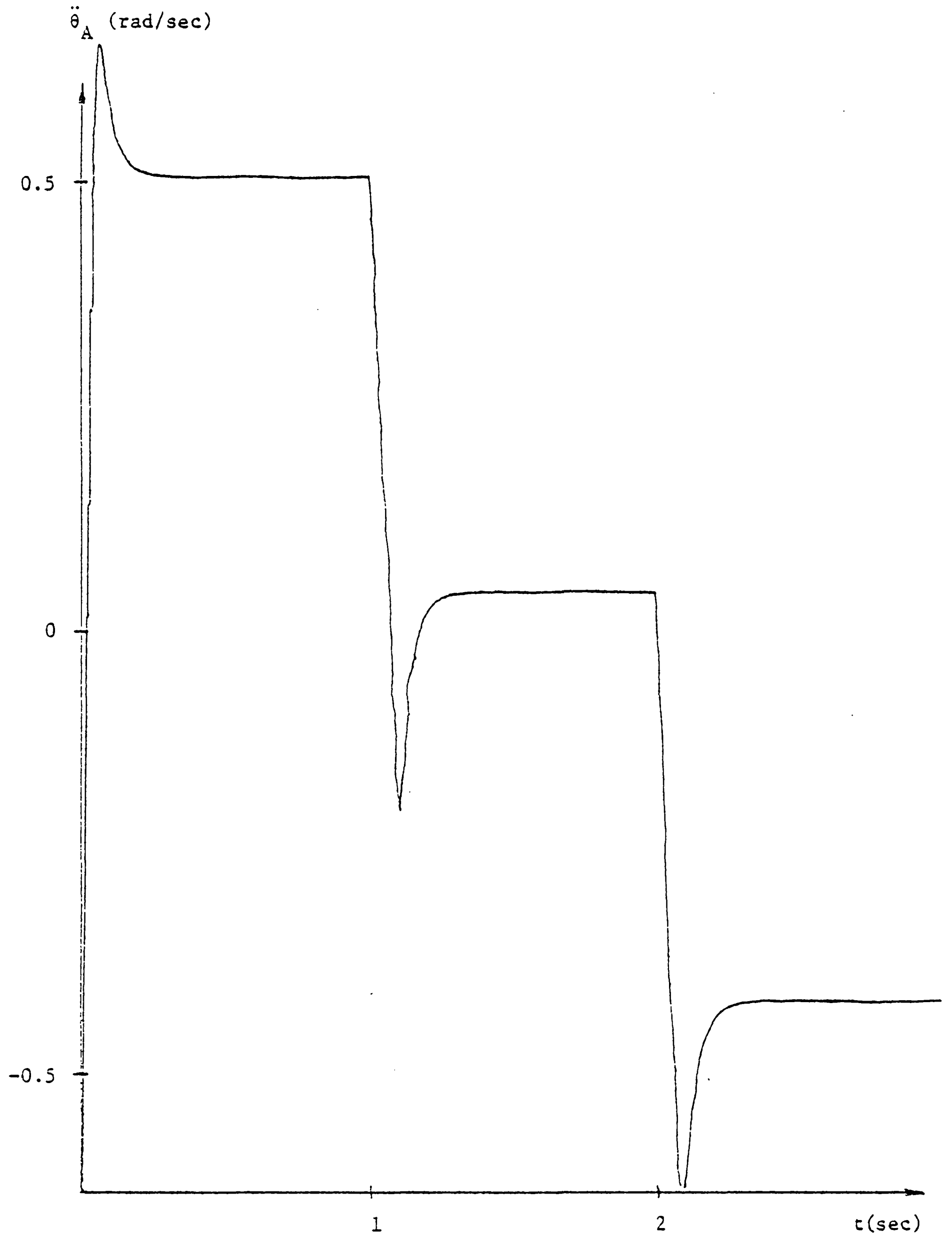

Fig. 3.12 Rate of Change of the Angular Position

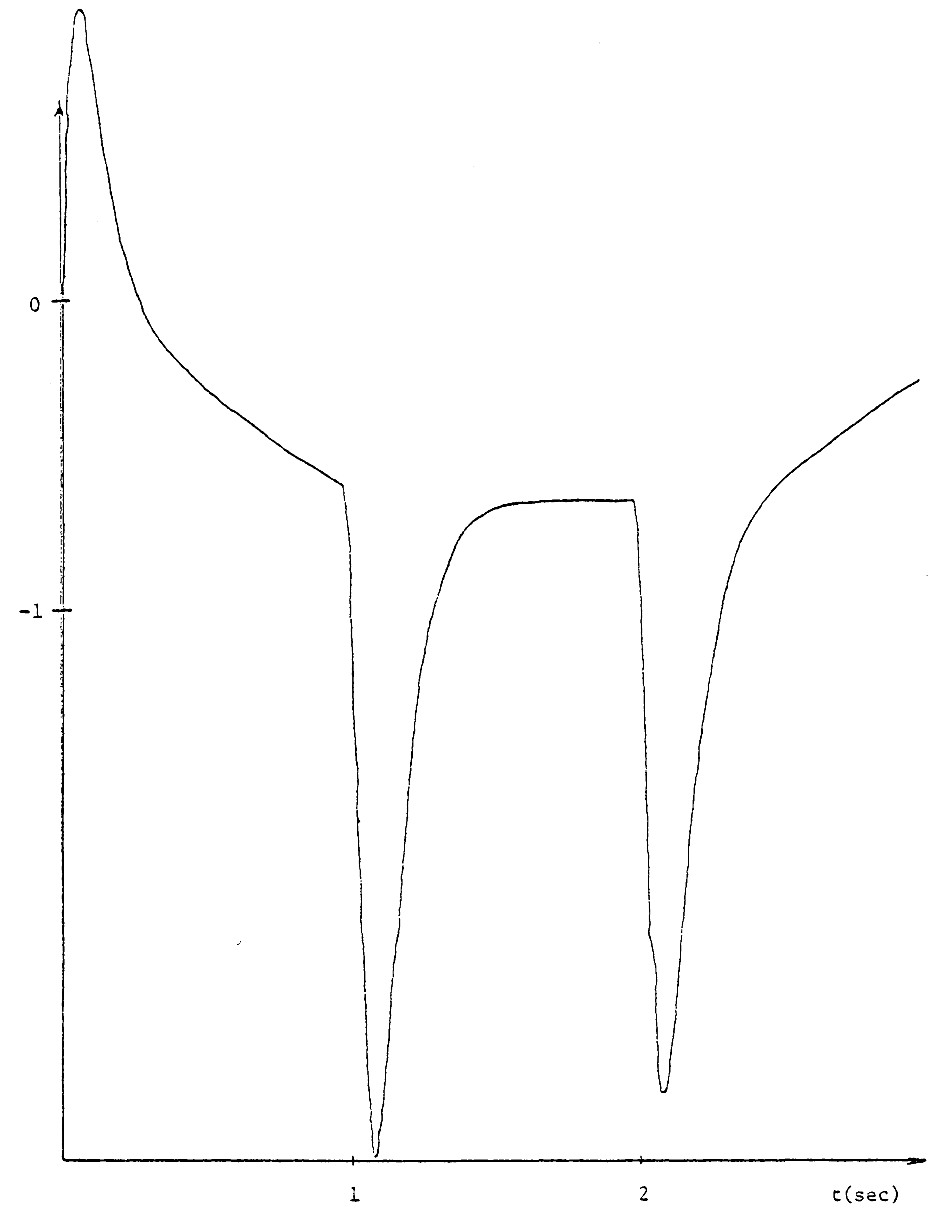

Fig. 3.13 "J. Hall" Output

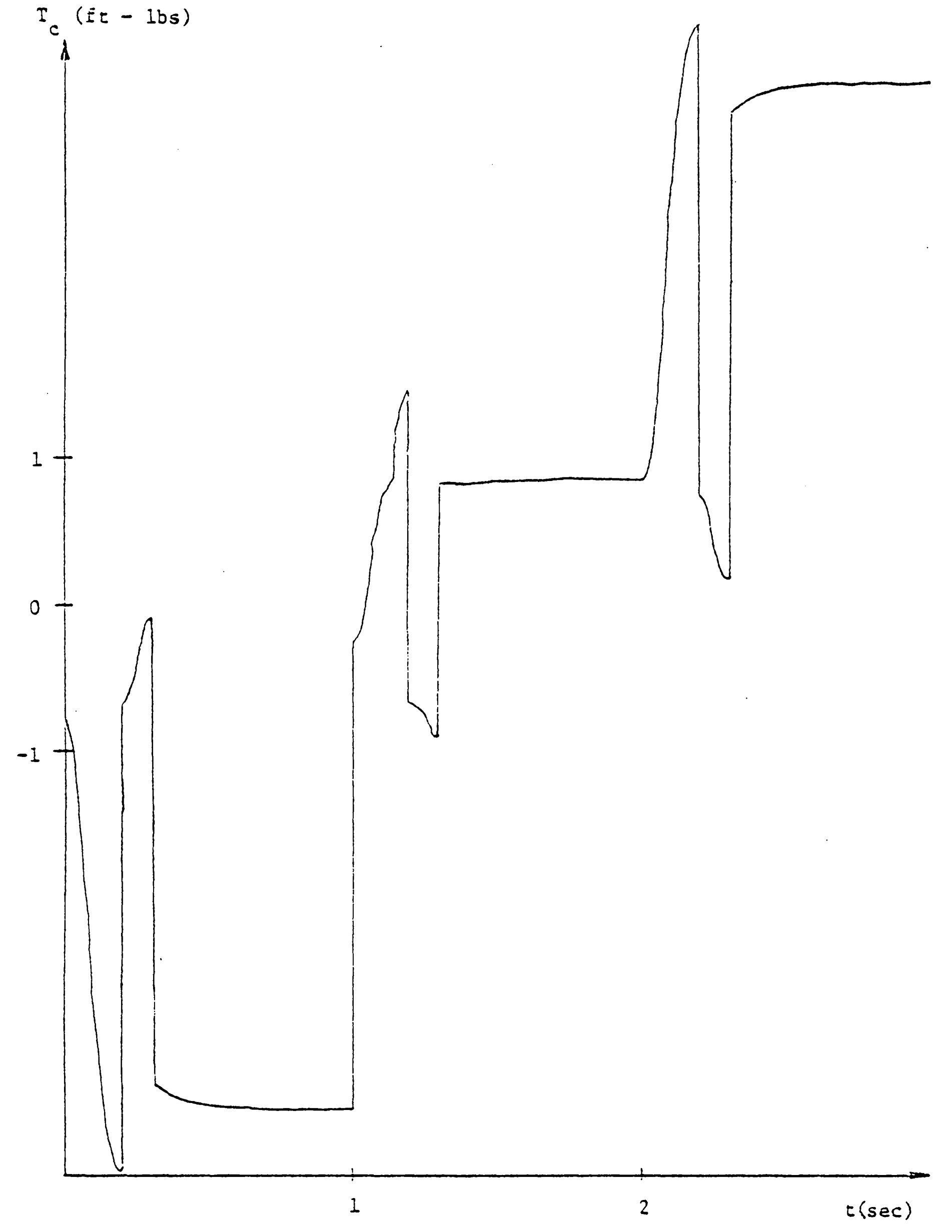

Fig. 3.14 Cable Torque

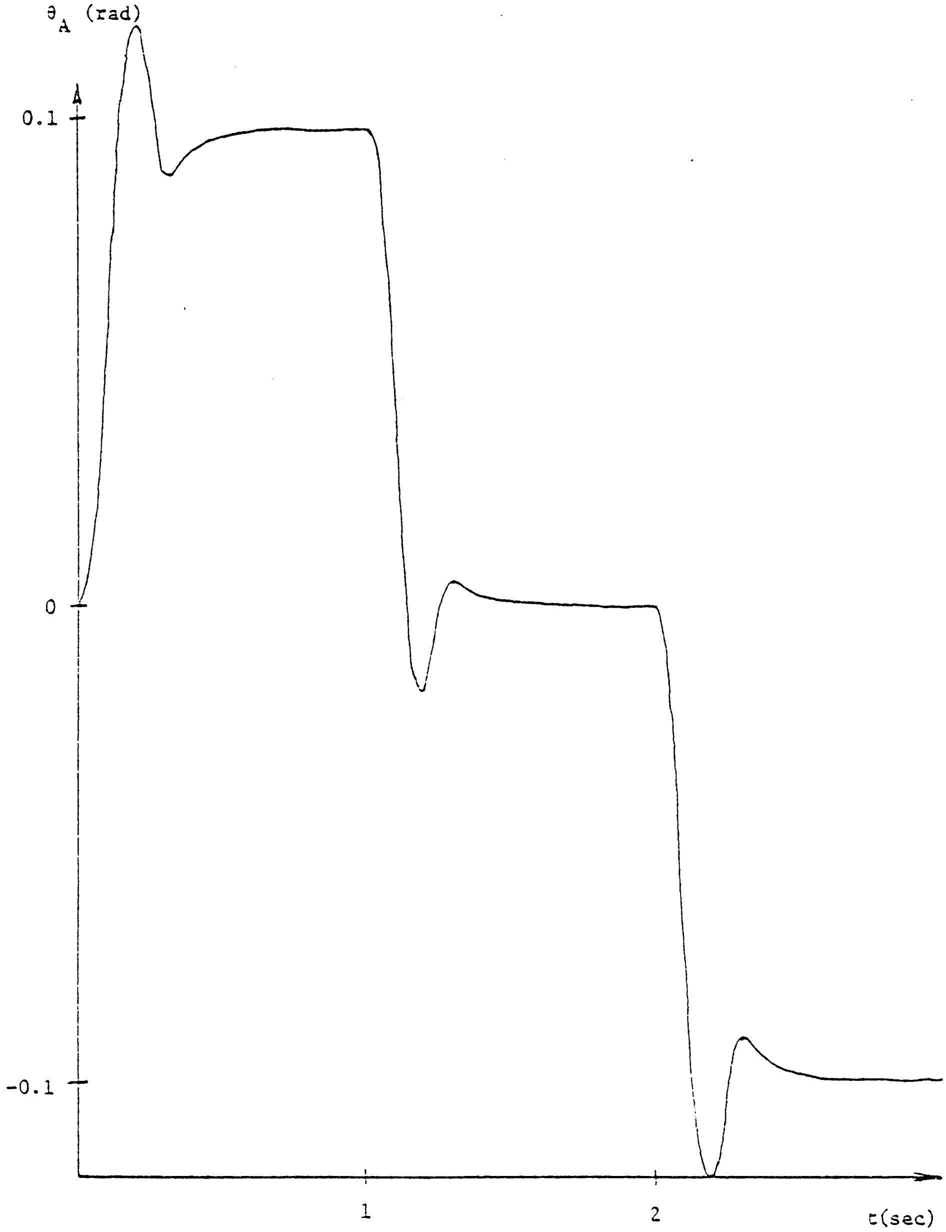

Fig. 3.15 Angular Position

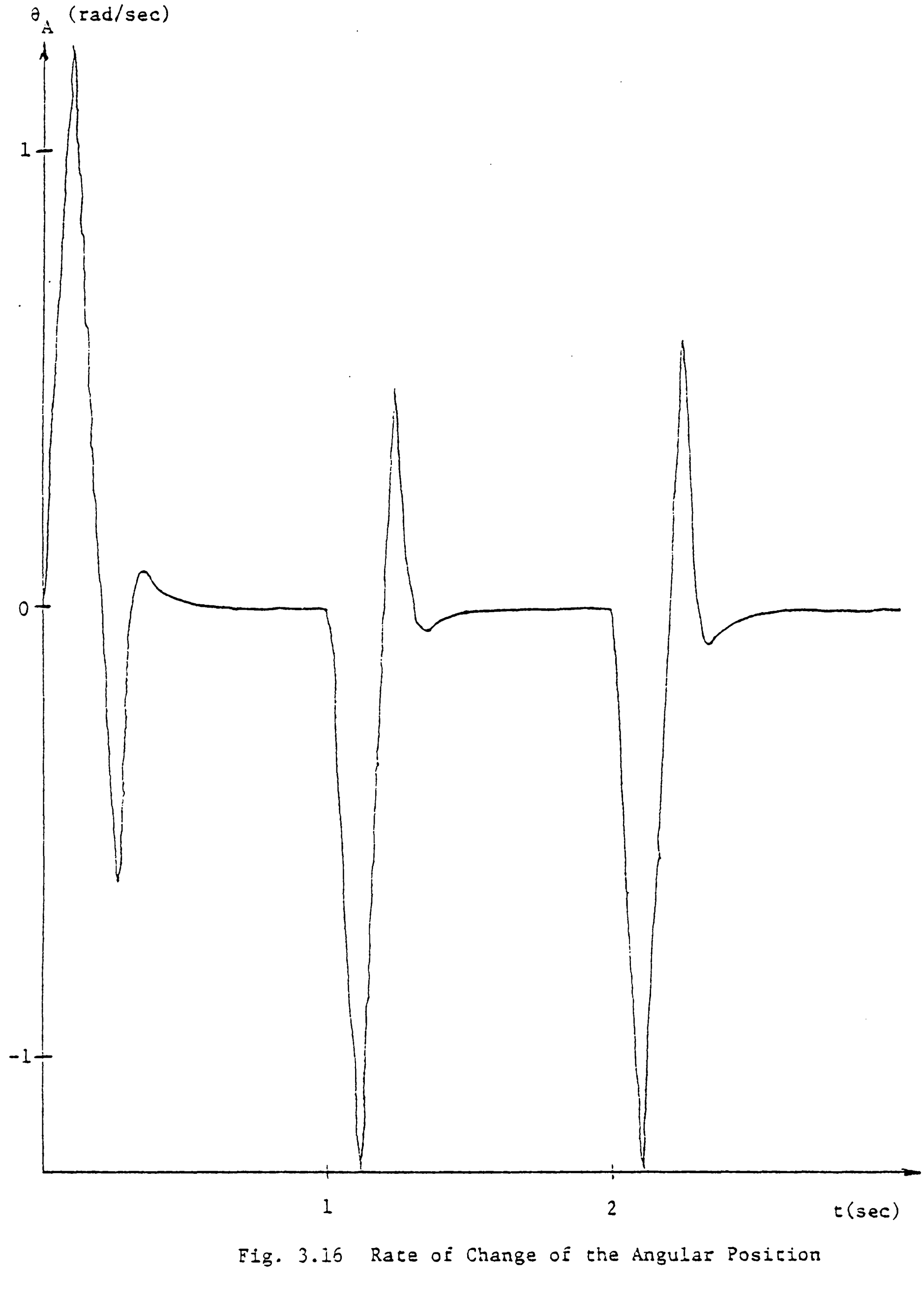

Fig. 3.16 Rate of Change of the Angular Position

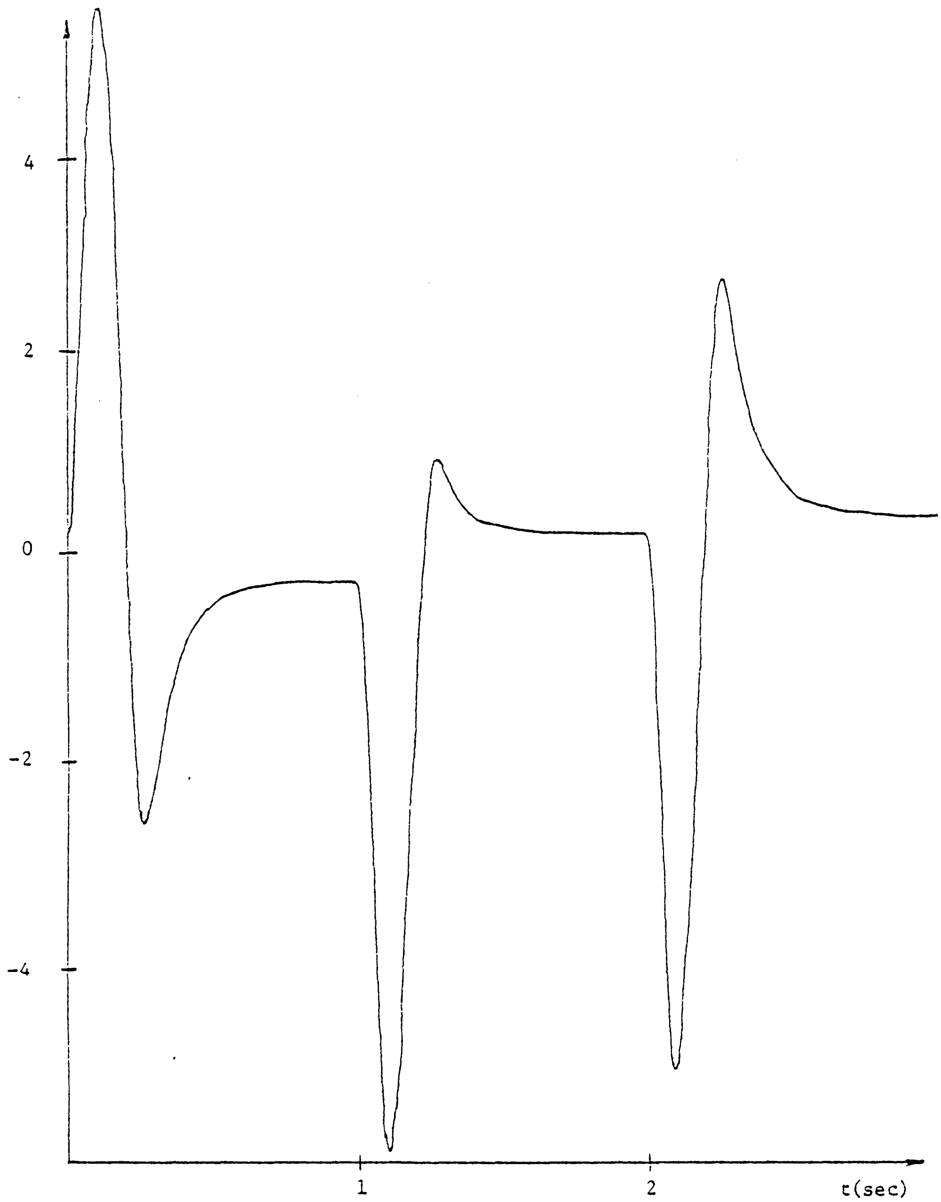

Fig. 3.17 "J. Hall" Output

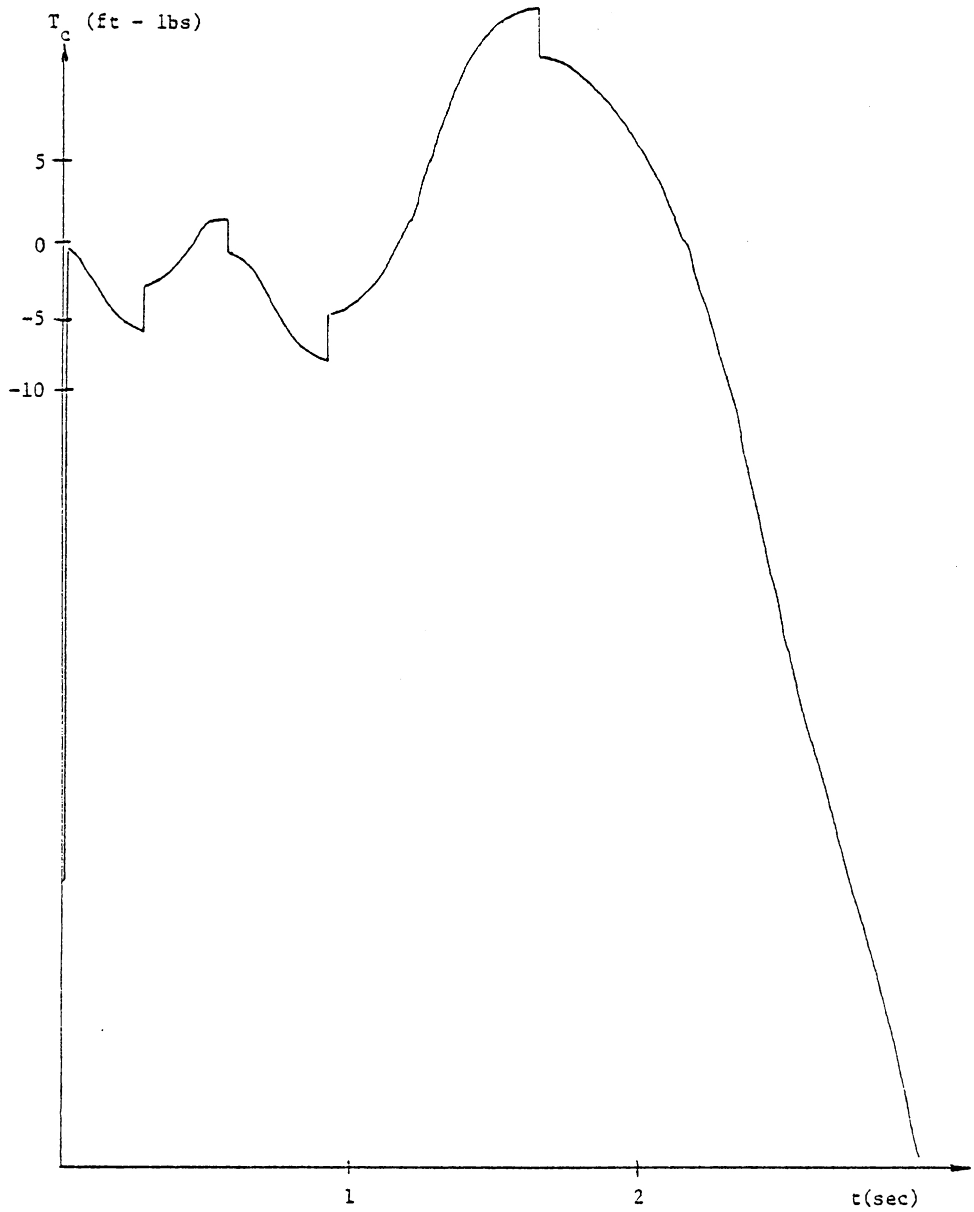

Fig. 3.18 Cable Torque

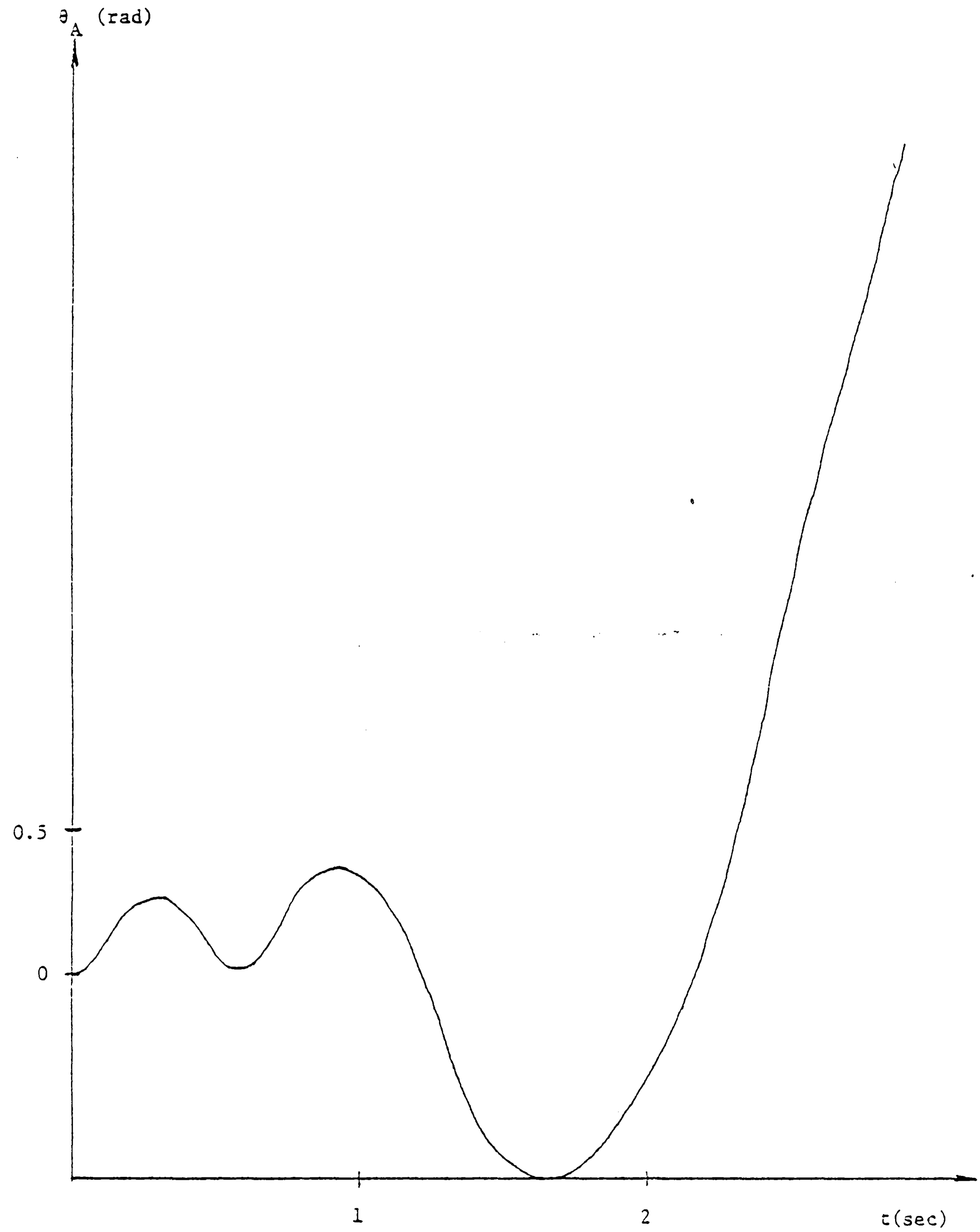

Fig. 3.19 Angular Position

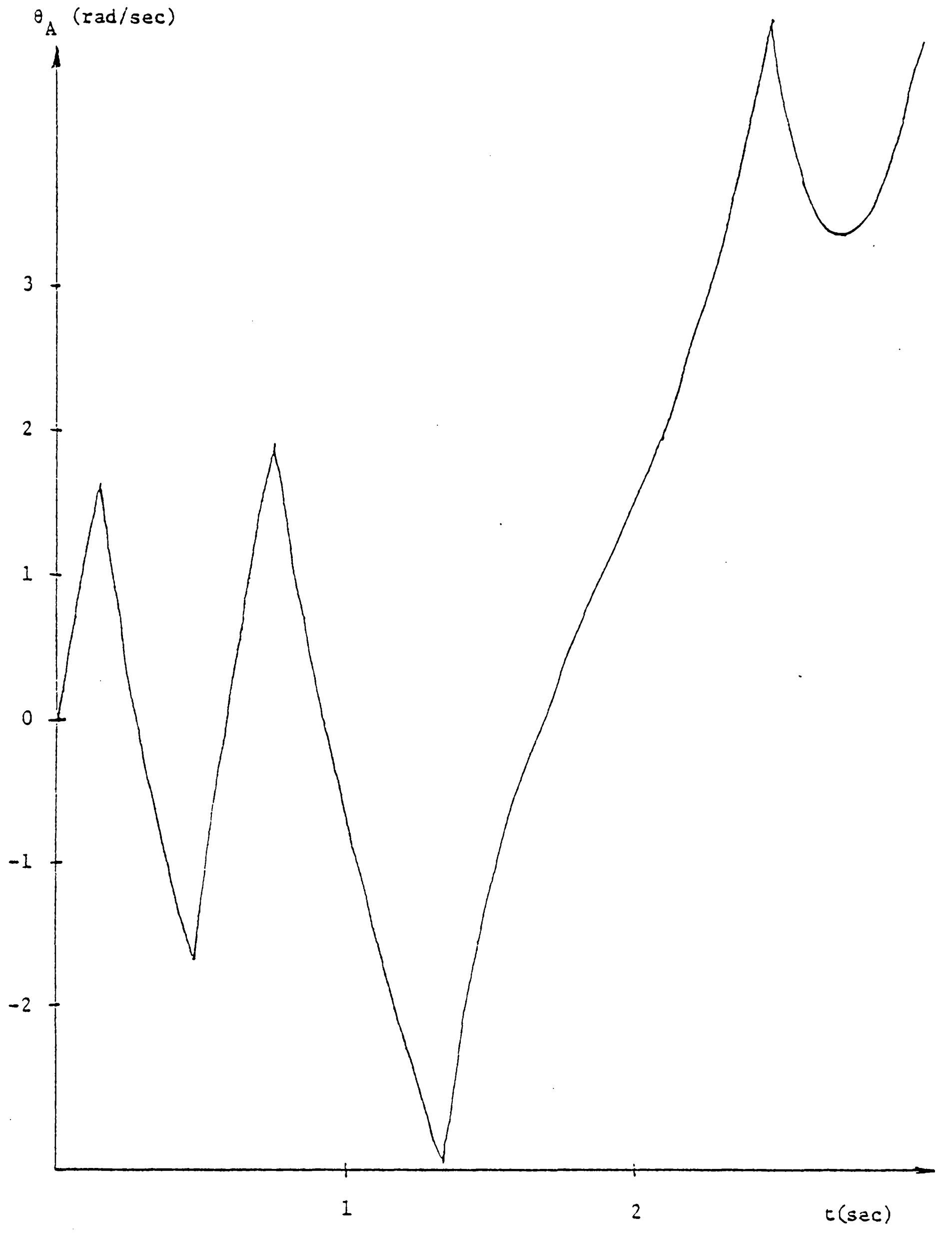

Fig. 3.20 Rate of Change of Angular Position

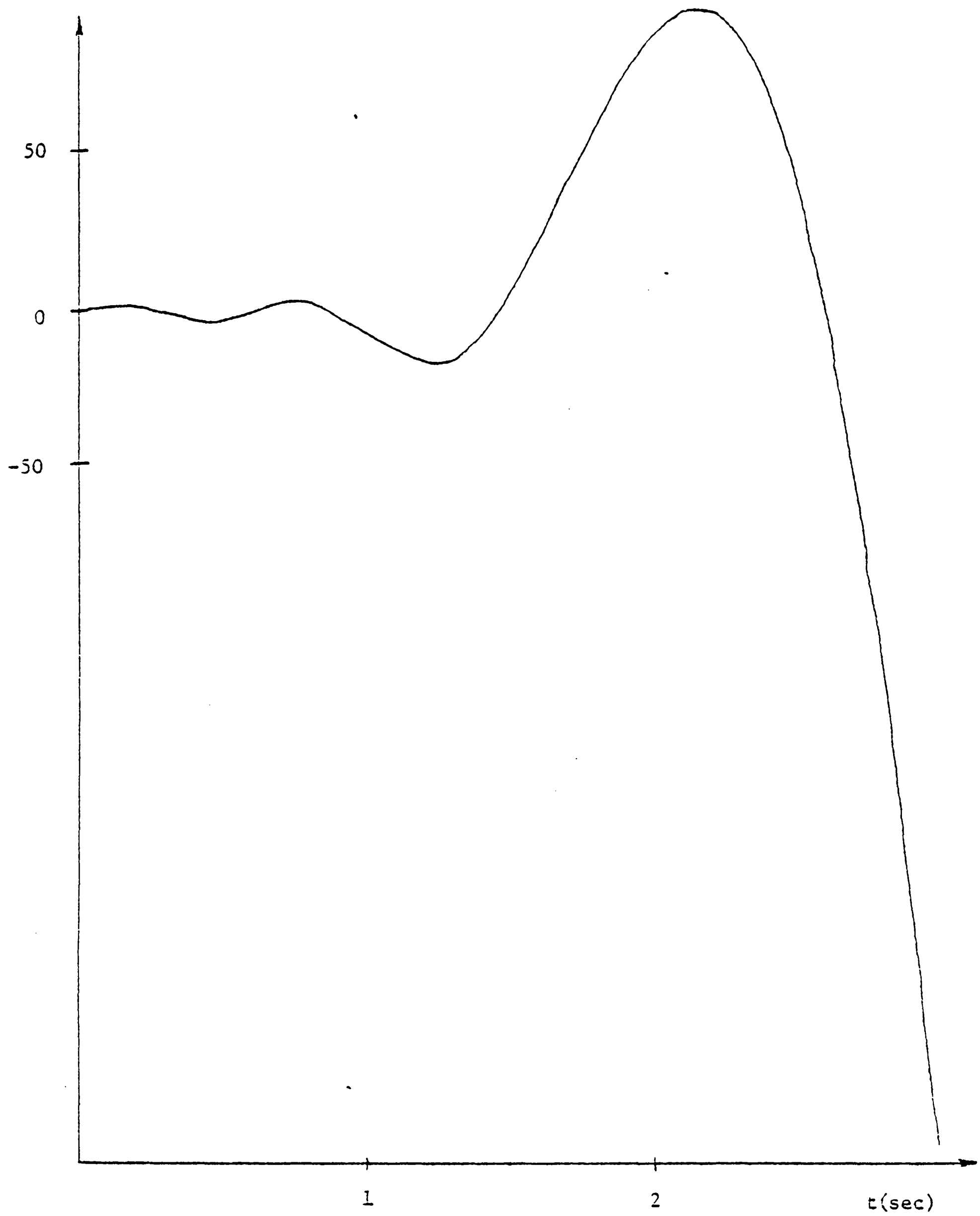

Fig. 3.21 "J. Hall" Output

4.0 CONCLUSIONS

A digital simulation technique has been shown to be successful when applied to the solution of nonlinear systems containing both deterministic and random inputs. Two closed-loop control system examples and a communication system problem have been presented. The results compared very favorably, and with a minimum amount of effort, with earlier published material which makes use of either complicated analytic quasi-linearizations, phase-plane techniques, or high speed analog computers. The simulation utilizes both the discrete-time state variable approach, and a sample-clamp operation around each nonlinearity that appears.

This method will handle large scale nonlinear, multi-input, multi-output systems and gives the designer a rapid indication of system behavior, that is, response times, stability for various input signal levels, etc., which are extremely difficult or impossible to achieve using standard analytical approaches.

REFERENCES

[1] Laning, J. H. and R. L. Battin, Random Processes in Automatic Control, McGraw-Hill, New York, 1956.

[2] Newton, G. C., L. A. Gould and J. F. Kaiser, Analytic Design of Linear Feedback Controls, John Wiley and Sons, Inc., New York, 1957.

[3] Papoulis, A., Probability Random Variables and Stochastic Processes, McGraw-Hill Book Co., 1965.

[4] Sage, A. P. and J. L. Melsa, Estimation Theory, McGraw-Hill Book Co., New York, 1971.

[5] Gelb, A. et al, Applied Optimal Estimation, The M.I.T. Press, Cambridge, MA., 1974.

[6] Smith, H. W., Approximate Analysis of Randomly Excited Nonlinear Controls, M.I.T. Press, Cambridge, MA., 1966.

[7] Gibson, J. E., Nonlinear Automatic Control, McGraw-Hill Book Co., New York, 1963.

[8] VanTrees, H. L., Synthesis of Optimum Nonlinear Control Systems, M.I.T. Press, Cambridge, MA., 1962.

[9] Wang, M. C. and G. E. Uhlenbeck, "On the theory of Brownian Motion", Rev. Mod. Phys., Vol. 17, April and July 1945.

[10] Kuo, B. C., Discrete-Data Control Systems, Prentice-Hall, Inc., Englewood Cliffs, N.J., 1970, pp. 122-123.

[11] Cadzow, J. A. and H. R. Martens, Discrete-Time and Computer Control Systems, Prentice-Hall, Englewood Cliffs, N.J., 1970.

The vita has been removed from the scanned document

COMPUTER SIMULATION OF A LARGE-SCALE

NONLINEAR FEEDBACK CONTROL SYSTEM

(ABSTRACT)

The computer simulation language written in Fortran was used to model the Navy's PHALANX Mount and Antenna Compensation Network. This network is a feedback control system that filters out the effects of surface ship motion on a weapon's response to commands from the ship's fire control center. The network includes a number of non-standard elements that prevent mathematical prediction of its closed-loop response; therefore, a computer model was required to predict the network's output.

The computer models were developed, validated and tested with a number of different inputs. The resultant outputs were compared with actual test data taken from a functional PHALANX mount compensation network.

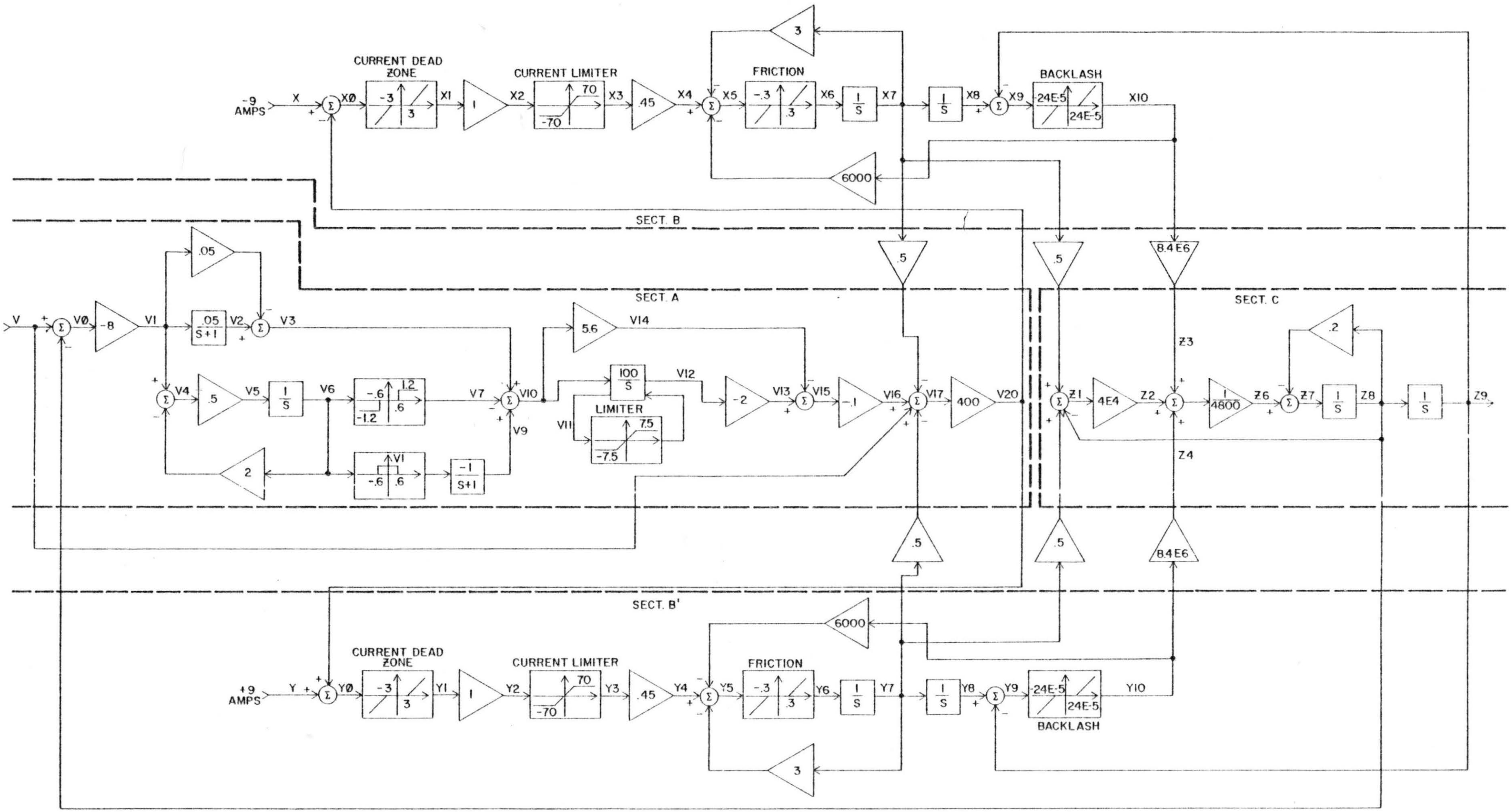

FIGURE I. PHALANX MOUNT COMPENSATION NETWORK